Synthesis of Chromophore-Catalyst Systems with Surface Anchoring Groups based on Perylene and Naphthalimide Towards Artificial Photosynthesis

Kirti Devi

A dissertation submitted for the partial

fulfillment of BS-MS dual degree in science.

Indian Institute of Science Education and Research, Mohali

April 2021

Certificate of Examination

This is to certify that the dissertation titled "**Synthesis of Chromophore-Catalyst Systems with Surface Anchoring Groups based on Perylene and Naphthalimide Towards Artificial Photosynthesis**" submitted by **Miss. Kirti Devi** (Reg. No. MS16091) for the partial fulfillment of BS-MS dual degree program of the Institute, has been examined by the thesis committee duly appointed by the Institute. The committee finds the work done by the candidate satisfactory and recommends that the report be accepted.

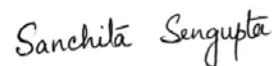Dr. Sugumar Venkataramani

Associate Professor

IISER Mohali

Dr. Raj Kumar Roy

Assistant Professor

IISER Mohali

Dr. Sanchita Sengupta

Assistant Professor

IISER Mohali

(Supervisor)

Dated: April 30, 2021

Declaration

The work presented in this dissertation has been carried out by me under the guidance of Dr. Sanchita Sengupta at the Indian Institute of Science Education and Research Mohali.
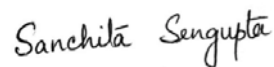
This work has not been submitted in part or in full for a degree, a diploma, or a fellowship to any other university or institute. Whenever contributions of others are involved, every effort is made to indicate this clearly, with due acknowledgement of collaborative research and discussions. This thesis is a bonafide record of original work done by me and all sources listed within have been detailed in the bibliography.

Kirti Devi

MS16091

Dated: April 30, 2021

In my capacity as the supervisor of the candidate's project work, I certify that the above statements by the candidate are true to the best of my knowledge.

Dr. Sanchita Sengupta

(Supervisor)

Acknowledgement

I would like to sincerely thank Dr. Sanchita Sengupta, my thesis supervisor, for allowing me to work in her lab. I am grateful for the guidance and support she gave me towards the completion of this project. I believe the experience I obtained under her supervision is instrumental in guiding my career.

I wish to thank my committee members Dr. Sugumar Venkataramani and Dr. Raj Kumar Roy for evaluating the work and giving valuable suggestions.

I would also like to express my gratitude to IISER Mohali for facilities and financial support for conducting the research.

I would like to express my deepest gratitude to my lab members Kavita, Narendra, Sushil, Anita, and Rosmi for their help, support and useful suggestions throughout the project. Thanks for keeping me motivated and providing a friendly atmosphere.

I want to thank all RKR group members (Umer, Deepak, Arjun, Ankita, Shubhendu, and Reena) for their help, support and maintaining a cheerful and comfortable atmosphere in the lab.

I am fortunate to have a family who believes in me and being the source of my strength and happiness. I'm really blessed to have each one of them in my life.

I would like to thank all my friends (in alphabetical order) Akshat, Anubhav, Bharath, Chahat, Divya, Parth, Saksham, Samyak, Sonell, Sparsh and Vishal who were there for me in my good and bad times and giving me best of these five years.

Table of Contents

List of Figures

List of Tables

List of Schemes

List of Abbreviations

AcOH - Acetic acid

APS - Artificial photosynthesis

ATP - Adenosine triphosphate

BET - Back electron transfer

BODIPY - 4,4-difluoro-4-bora-3a,4a-diaza-s-indacene

Br_2 - Bromine

BuBr – 1-Bromobutane

BuOH – 1- Butanol

^{13}C NMR – 13 Carbon NMR

$CDCl_3$ - Deuterated chloroform

CH_2Cl_2 - Dichloromethane

$CHCl_3$ - Chloroform

Cp^*IrCl_2 - Pentamethylcyclopentadienyliridiumdichloride

18-C-6 - 18-Crown-6

DSPEC - Dyesensitized photoelectrochemical cell

DMF - N,N-Dimethyl formamide

DBU - 1,8-Diazabicyclo(5.4.0)undec-7-ene

EtOH- Ethanol

FRET - Förster resonance energy transfer

^1H-NMR - Proton NMR

HOMO - Highest occupied molecular orbital

H_2 - Hydrogen

K_2CO_3 - Potassiumcarbonate

LUMO - Lowest unoccupied molecular orbital

MeCN - Acetonitrile

NADPH - Nicotinamide adenine dinucleotide phosphate

$NaHCO_3$ - Sodium bicarbonate

Na_2CO_3- Sodium carbonate

Na_2SO_4 – Sodium sulfate

NMP - N-Methyl-2-Pyrrolidone

NMR - Nuclear magnetic resonance

NPS – Natural photosynthesis

O_2 - Oxygen

PDI - Perylenediimide

PEC - Photoelectrochemical cell

PCET – Proton coupled electron transfer

$Pd(PPh_3)_4$ – Tetrakis(triphenylphosphine)palladium(0)

PhMe - Toluene

Pt - Platinum

RT - Room temperature

Ru - Ruthenium

RuO - Ruthenium oxide

SA-N-P-N - Surface anchoring-naphthalimide-perylene-naphthalimide

TiO_2 - Titanium dioxide

TLC - Thin layer chromatography

TsOH - p-toluene sulphonic acid

WOC - Water oxidation catalyst

Zr - Zirconium

Abstract

The aim of this work is to synthesize a light-harvesting antenna synthetically functionalized with water oxidation catalyst (WOC) as well as a chromophore-catalyst assembly to achieve photocatalytic water oxidation into a more straightforward artificial photosynthesis system. Multiple chromophores capture light energy and transfer this energy into a central chromophore by a process called Forster resonance energy transfer (FRET). The judicious selection of energy donor chromophore and energy acceptor chromophore determines the light-harvesting antennae's energy transfer efficiency. The selection of energy donor chromophore and energy acceptor chromophore governs the efficiency of the LH antennae. In this work, two multichromophore catalyst systems were designed and synthesized in part. The molecules were functionalized with surface anchoring (SA) groups attached to the central perylene (P) chromophore that is functionalized with naphthalimide (N) chromophores at bay positions to design: (a) SA-N-P-N system and (b) SA-N-P-N-catalyst system, where Iridium based water oxidation catalyst will be covalently attached to the SA-N-P-N system in the final synthetic step. In both systems, perylene was chosen as the central energy acceptor and naphthalimide as peripheral energy donor as the near-quantitative spectral overlap of emission of naphthalimide donor and absorption of perylene acceptor render them one of the most efficient FRET pairs. Efficient FRET leads to rapid migration of excitation energy to the central chromophore from the peripheral chromophores and, as a result, leads to rapid charge separation and prevents back electron transfer (BET), two of the most vital processes that decide the efficiency of an artificial photosynthesis system. The prevention of BET is a significant parameter in improving such artificial photosynthetic systems' overall efficiency.

Chapter 1

Introduction

The sustainable production of clean energy constitutes one of the most critical scientific challenges of the 21st century. A significant part of the global energy supply is provided by carbon-based energy sources (fossils fuels) connected to severe environmental issues, such as air pollution and the greenhouse effect. Moreover, there is a possibility of the scarcity of fossil fuels in the coming years. Consequently, there exists a strong demand for clean and environment-friendly carbon-neutral energy alternatives. Every hour of sunlight provides our planet with more energy than consumed during a whole year. This fact has mesmerized researchers looking for better ways to convert solar energy into fuel and electricity to solve the impending energy crisis. An excellent way to approach this energy demand and reduce carbon footprint due to fossil fuel usage is through the judicious design of photochemical cells.[1]

A solar energy conversion device collecting and converting all of the sunlight striking just 2% of the earth's surface for 8 hr with an energy conversion efficiency of 12% would be sufficient to satisfy global energy consumption for two weeks.[2] Today, photovoltaics (PV) are produced on commercial scales that can directly convert solar energy into electricity. The solar energy harvested in PV devices can be stored in external batteries. The most efficient and lightweight batteries are typically Li$^+$ batteries. However, considering energy demand in today's world, Li$^+$ ion battery technology will not meet global energy storage demands. The design of artificial solar light-harvesting systems that mimic all the natural photosynthesis events in dye-sensitized photo electrochemical cell (DSPEC) device configuration will be an excellent alternative strategy production of hydrogen fuel in a sustainable way. Artificial photosynthesis offers a way to overcome the challenges as mentioned above.

1.1. Natural Photosynthesis

In natural photosynthesis, plants use direct sunlight to reduce CO_2 by water to make carbohydrates and oxygen with energy stored as adenosine triphosphate (ATP). However, photosynthesis is inefficient, converting only ~1% of the incident sunlight into biomass, with the remainder being used for signaling, growth, and other energy demands.[1] The photosynthetic apparatus (Figure 1) uses solar energy to reduce CO_2 to carbohydrates (here represented as

$C_6H_{12}O_6$) according to eq 1.[1] The natural system constitutes an excellent source of inspiration for how to design a system that can utilize solar energy for fuel production.

$$6CO_2 + 12H_2O \rightarrow C_6H_{12}O_6 + 6O_2 + 6H_2O \qquad\qquad (1)$$

The light reaction of natural photosynthesis (NPS) occurs via a series of step-wise electron-transfer processes to create sufficient water-splitting energy. This process, known as the "Z-scheme," is shown in Figure 1.1. Two photosystem - photosystem I (PSI) and photosystem II (PSII) – collect light energy through an assembly of light-harvesting chlorophylls and transfer electrons to a higher electronic state (excitation) inside a reaction center. These photosystems are connected in series with various electron acceptors, which are arranged according to their oxidation potential like the letter "Z"; therefore, figure 1.1 is also known as the "Z" scheme of natural photosynthesis. [1]
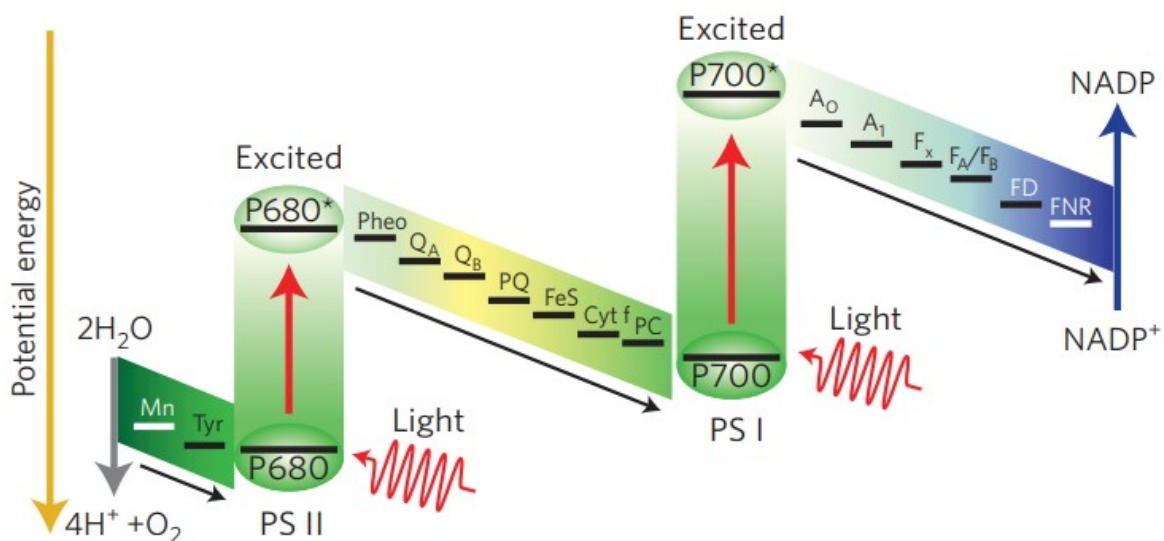
Figure 1.1. NPS charge-separation processes, including type I and II reaction centers (simplified Z-scheme). P680: pigment (chlorophyll) that absorbs 680 nm light in photosystem II (PSII); P680*: the excited state of P680; P700: pigment (chlorophyll) that absorbs 700 nm light in photosystem I (PSI); P700*: the excited state of P700. Mn: manganese calcium oxide cluster; Tyr: tyrosine in PSII; Pheo: pheophytin, the primary electron acceptor of PSII; QA: primary plastoquinone electron acceptor; QB: secondary plastoquinone electron acceptor; PQ: plastoquinone; FeS: Rieske iron sulphur protein; Cyt. f: cytochrome f; PC: plastocyanin; A_0: primary electron acceptor of PSI; A_1: phylloquinone; F_X, F_A, F_B: three separate iron sulphur centers; FD: ferredoxin; FNR: nicotinamide adenine dinucleotide phosphate (NADP) reductase. Courtesy: *Nature Photon* **6,** 511–518 (**2012**).[3]

This Z-scheme process is driven by the absorption of two photons, one at PSII and the other at PSI. Light absorption at PSII creates P680*, which provides an electron to reduce pheophytin, and the step-wise electron transfer occurs from pheophytin to $P700^+$ (the oxidizing species after the electron transfer from P700*). Following this initial electron transfer, $P680^+$ can oxidize tyrosine and subsequently the manganese calcium oxide cluster. Light absorption at PSI creates P700*, which provides an electron to reduce A_0 (primary electron acceptor to FNR. Black arrows indicate a series of electron transfer pathways.[3]

1.2. Artificial Photosynthesis

The creation of artificial systems for the generation of fuels from sunlight, based on natural photosynthesis principles, can be described as creating an "artificial leaf". Artificial photosynthesis results in the formation of hydrogen from water splitting or carbon-based fuels such as methanol etc, resulting from CO_2 reduction. This is a photo-driven process, whereby the energy is stored as, for example, H_2, which is produced from the reduction of protons generated from the oxidation of H_2O. The success of artificial photosynthesis is mainly dependent on the ability of artificial photosynthetic devices to collect the maximum amount of incident sunlight followed by the cascade of electron transfer processes to eventually generate molecular oxygen and hydrogen from water.[4]

The first component in such a molecular level device is a light-harvesting antenna. Artificial light-harvesting antennae consist of multiple chromophores with distinct chemical structures and complementary absorption features, enabling them to harvest the maximum amount of sunlight covering the maximum region across the visible part of the solar spectrum (i.e., 400-700 nm range). These multiple chromophores absorb light energy and, if properly designed, can transfer the harvested excitation energy to a central chromophore by unidirectional energy transfer, a funneling effect through an energy transfer mechanism known as Förster resonance energy transfer (FRET). For the energy transfer to occur efficiently through FRET, the electronic properties of all the chromophores in light-harvesting antenna should be complementary to each other.[5]

In an artificial photosynthetic system, it is thus essential to devise an efficient process that (1) can efficiently absorb light through chromophores (photosensitizer), (2) form a charge-separated

state by transferring the electron to a reduction catalyst, usually via a primary acceptor, (3) accept and accumulate two consecutive electrons at the reduction catalyst to subsequently use these to reduce two protons to molecular hydrogen, (4) allows regeneration of the chromophore by transfer of an electron from the oxidation catalyst, generally, via a primary donor, and (5) after transfer of four consecutive electrons, one by one, from the oxidation catalyst, the oxidation catalyst is regenerated by a formal one-step transfer of four electrons from two molecules of H_2O to generate one molecule of O_2 and four protons.[4]
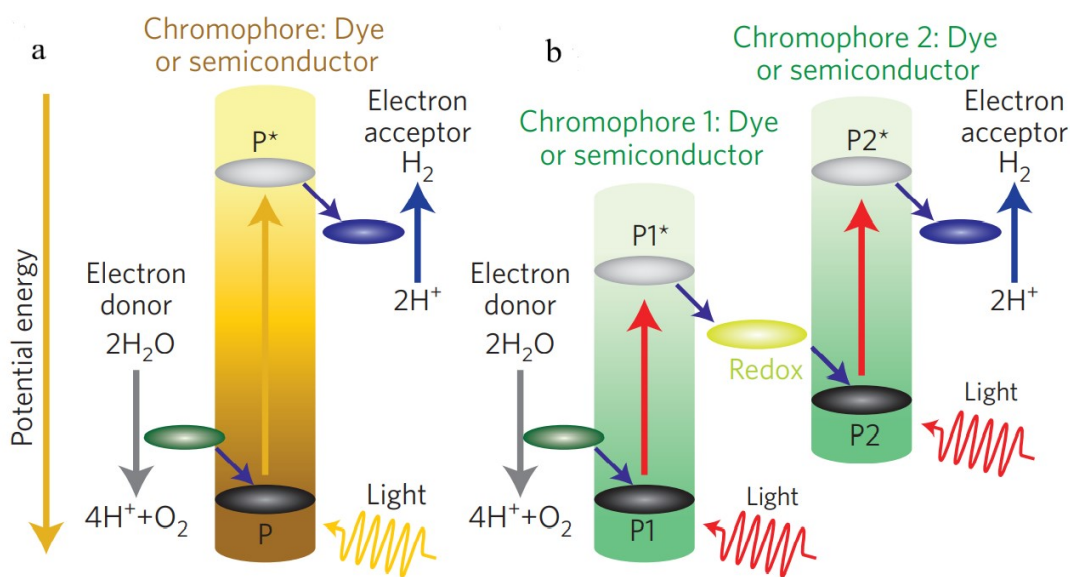
Figure 1.2. Artificial photosynthesis charge-separation process (a) single step reactions and (b) two-step (Z) reactions. P: chromophore of a single-step reaction system; P*: excited state of P; P1: the first chromophore of a twostep reaction system; P1*: excited state of P1; P2: second chromophore of a two-step reaction system; P2*: excited state of P2. Courtesy: *Nature Photon* **6,** 511–518 (**2012**).[3]

For APS systems, two different types of material structures are currently accepted. Figure 1a shows the first, which comprises a single light-excitation site attached to an electron donor on one side and an electron acceptor on the other. The two-step process (Fig. 1b) is an alternative technique that is analogous to the NPS Z-scheme. One advantage of the two-step process is that it can utilize lower energy sunlight (down to near-infrared wavelengths) and thus increase available material combinations. As long as the excited-state oxidation potential at the oxygen-evolving site (P1* in Fig. 1c) is more negative than the excited state reduction potential at the hydrogen-evolving site (P2), there is no further potential requirement for these states. However,

the overall system structure is more complex than that of the single-step process. For example, in the two-step process, it is more difficult to control the kinetic balance for the whole electron-transfer process without losing the energy through charge recombination reactions.[3]

1.3. Photoelectrochemical (PEC) cells

The artificial photosynthetic target of water splitting to give hydrogen is shown in eq 2, and solar-driven reduction of CO_2 by water to give to the 2e- product formic acid is shown in eq 3. More highly reduced carbon targets are an ultimate goal; reduction to methanol is shown in eq 4.

$$2H_2O \rightarrow O_2 + 2H_2 \tag{2}$$

$$H_2O + CO_2 \rightarrow HCOOH + O_2 \tag{3}$$

$$2H_2O + CO_2 \rightarrow CH_3OH + O_2 \tag{4}$$

In a photoelectrochemical cell, the reactions in eqs 2−4 are carried out by separate half-reactions for oxidation and reduction. The half-reactions for CO_2 reduction by H_2O to give HCOOH and CH_3OH are illustrated in eq. 3 and 4, respectively.[2]

Many device architectures were proposed for artificial photosynthesis.[2] Honda and Fujishima, for the first time in 1972, reported that water splitting into H_2 and O_2 occurred following ultraviolet (UV) excitation of anatase titanium dioxide (TiO_2) in a PEC cell with a Pt cathode and a small applied bias in acidic solution (Figure 1.3.). But this system was limited to UV light only, and a single material, TiO_2, was performing multiple functions like light absorption, water oxidation, charge generation, and transportation.[5] Such PECs had several limitations of BET, photo-corrosion, low efficiency, and most of the solar spectrum was not usable. Next, Grätzel and co-workers designed a PEC consisting of TiO_2 as a photoanode and RuO_2 as a water oxidation catalyst, and Pt as a cathode.[6] But the efficiency of this system was also low due to the rapid recombination of charge carriers. Bard described an architecture resembling the "Z" scheme of natural photosynthesis in 1979.[2] In photosynthesis, reduction of NADP to NADPH occurs at photosystem I (PSI) and water oxidation at photosystem II (PSII). Photosynthesis uses a tandem "Z-scheme," which integrates physically separated photochemical reactions. A tandem configuration offers far greater redox potentials for driving the separate half-reactions. In Bard

Tandem cell, water oxidation and reduction were driven at separate nanoparticle photocatalyst in solution.[3]
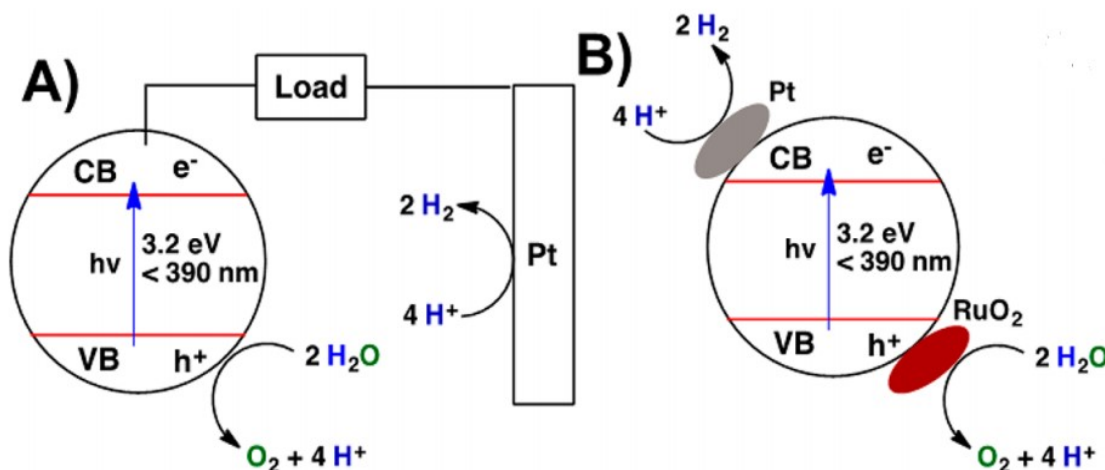
Figure1.3. (A) Honda-Fujishima model for photo electrochemical cell with TiO_2 as photoanode.[12] (B) Grätzel model of photo electrochemical cell illustrating semiconductor nanoparticle with RuO2 as the water oxidation catalyst and Pt as the reduction catalyst. Courtesy: *J.Am.Chem. Soc*.**1981** 103(16), pp.4685-4690. [2]

1.4. Water oxidation

In both natural and artificial photosynthesis, the thermodynamic, mechanistic, and kinetic requirements that arise from light-driven water oxidation pose a significant challenge. Because it is a four-electron process, water oxidation at moderate overpotential (100-300 mV) is slow even with the best catalysts. A related problem is that molecules that can oxidize water tend to be unstable at the very positive potentials needed to drive the reaction. Water oxidation catalysts must deliver electrons to oxidized photosensitizer molecules rapidly because the time scale for back electron transfer is fast, typically microseconds to milliseconds.[4]

A schematic overview of how a device for H_2O splitting can be constructed is depicted in figure1.4

Figure 1.4. Schematic picture of a molecular assembly for overall H_2O splitting consisting of a photosensitizer (PS), a water oxidation catalyst (WOC), and a hydrogen evolving catalyst (HEC), for the production of solar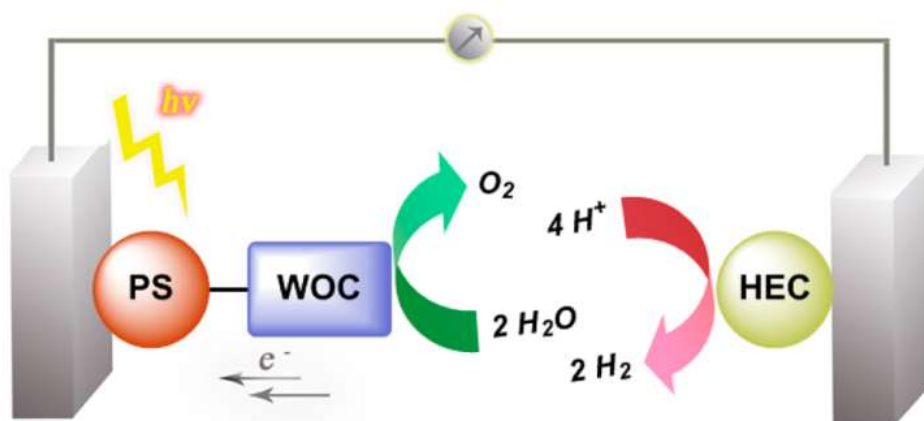 fuels. Courtesy: *Chem.Rev.* **2014** *114* (24), 11863-12001. Reprinted with permission from ref 3. Copyright 2014 American Chemical Society.

1.5. Dye-sensitized photo electrochemical cells (DSPECs)

A hybrid molecular-semiconductor approach based on dye-sensitized photoelectrochemical cells (DSPECs). It combines molecular-level light absorption and catalysis by chromophore-catalyst assemblies with stable wide-band-gap semiconductor oxides, either n-type (TiO_2, SnO_2, ZnO) or p-type (NiO). Water splitting in a DSPEC is initiated by light absorption by a surface-bound chromophore. In DSPEC for water splitting, injected electrons are used to reduce H^+/H_2O to H_2. Oxidative equivalents are accumulated at the catalyst in a chromophore-catalyst assembly for water oxidation.

The key elements of the DSPEC are:

(1) A nanostructured, mesoporous n-type semiconductor oxide electrode, transparent in the visible (Vis) region;

(2) A UV/visible light-harvesting chromophore which, upon excitation, forms an excited state or states which efficiently inject electrons in the semiconductor oxide;

(3) A water oxidation catalyst;

(4) A separate cathode where H_2O/H^+ is reduced to H_2.
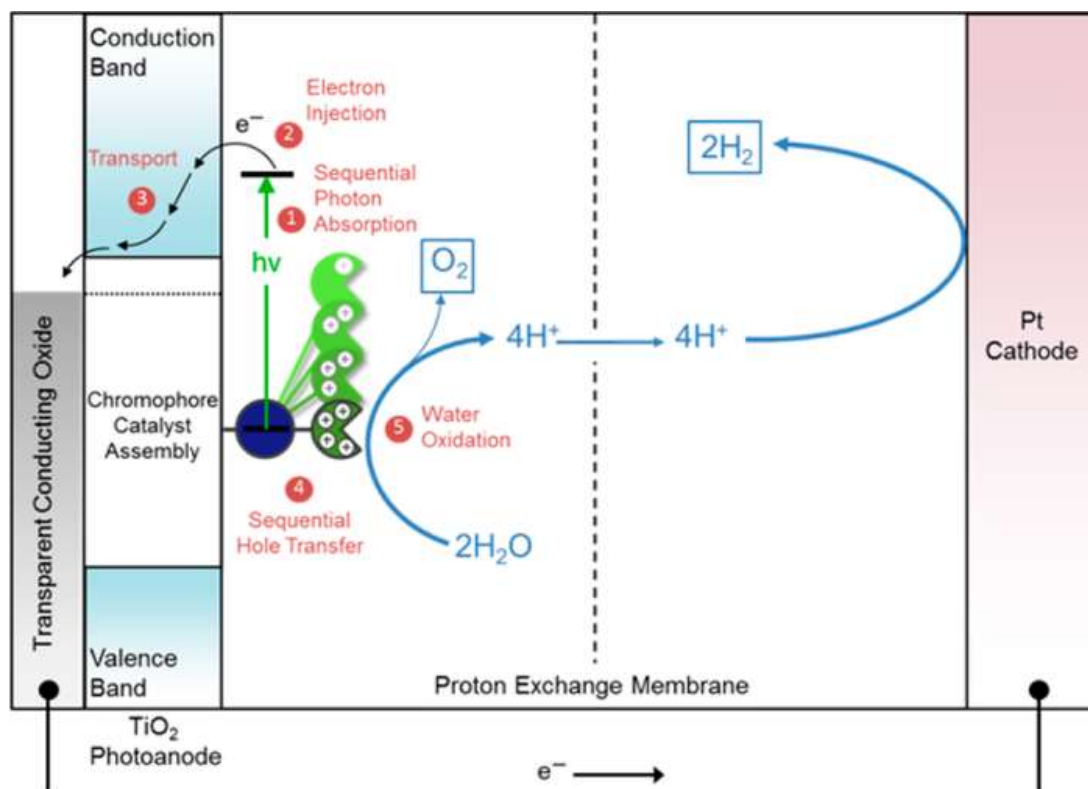
Figure 1.5. A sequence of water splitting in DSPECs into H_2 and O_2. Image courtesy: *Chem. Rev.* **2015**, 115, 13006−13049. Reprinted with permission from ref 2. Copyright 2015 American Chemical Society.

Charge carrier formation occurs at the surface of chromophores, and the working principle of a dye-sensitized photo electrochemical cell (Figure 1.5) consists of the following five steps:

1) Light absorption by chromophore that is attached to the semiconductor surface (photoanode).

2) Injection of excited electrons from the chromophore into the conduction band of the semiconductor.

3) Transfer of electrons from the conduction band of semiconductor to the photo anode with the application of a bias to drive H_2 production to completion

4) Intra-assembly electron transfer from the catalyst to chromophore activating the catalyst towards the water oxidation.

5) Repetition of steps 1−4 four times to drive water oxidation and oxygen evolution at the water oxidation catalyst, followed by H_2O/H^+ reduction to H_2 at the cathode.[2]

The efficiency of DSPECs depends upon the kinetics of electron transfer which further depends on band gap engineering and methods of assembling a light-harvesting system and catalyst on the metal oxide surface. Moreover, the highest occupied molecular orbitals (HOMO) - lowest unoccupied molecular orbital (LUMO) energy levels of dye, the conduction band of TiO_2, and WOC for efficient electron transfer should be aligned as shown in figure 1.6. in order to achieve the maximum efficiency of DSPEC.
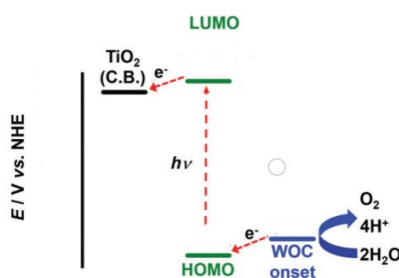
Figure 1.6. Energy level diagram showing HOMO-LUMO levels of the chromophore, oxidation potential of the water oxidation catalyst, and conduction band of TiO_2.[8]

1.6. Chromophore-catalyst assemblies

1.6.1. There are two design strategies generally adopted for the chromophore-catalyst assemblies:

1) **Co-adsorption:** In the co-adsorption strategy, both chromophore and the water oxidation catalyst are separately functionalized and are attached to the metal oxide surface separately. The electron or hole transfer from catalyst to chromophore or vice versa occurs mainly through space.

2) **Covalently linked chromophore catalyst system:** In this design, as depicted in figure1.8, the chromophore and the water oxidation catalyst are covalently connected through a bridging ligand, and they are functionalized with a surface anchoring group that can bind to the metal oxide surface (photoanode). The electron or hole transfer from a catalyst to a chromophore or vice versa occurs through a bond or space—the bridging ligand between the chromophore and the catalyst help with rapid intra assembly electron transfer.
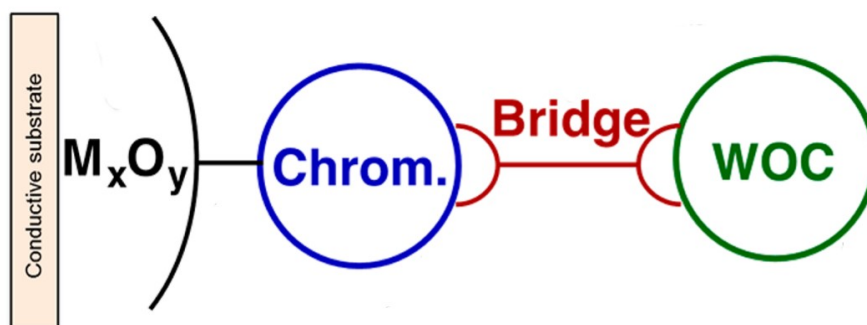
Figure 1.8. A covalently linked DSPEC chromophore-catalyst assembly. This consists of a water oxidation catalyst that is linked to ch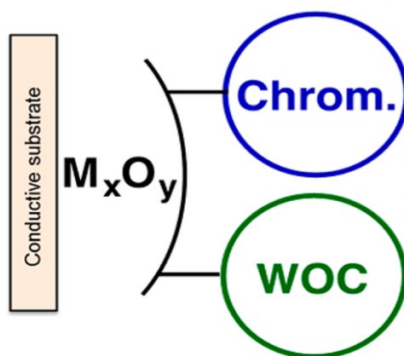romophore by a bridging ligand. This whole system was functionalized with metal oxide by an anchoring group. Courtesy: *Chem. Rev.* **2015**, 115, 13006−13049. Reprinted with permission from ref 2. Copyright 2015 American Chemical Society.

1.6.2. Literature examples of chromophore-catalyst assemblies

In practical DSPEC candidates, the use of inexpensive organic dyes and first-row transition metal complex catalysts for water oxidation is clearly desirable, based on cost and abundance. The first designed molecular catalyst for water oxidation was Ru(III) "blue dimer", cis, cis-$[(bpy)_2(H_2O)Ru^{III}ORu^{III}(OH_2)(bpy)_2]^{4+}$ Figure 1.9.[2] It undergoes PCET activation to give $[(bpy)_2(O)Ru^{V}ORu^{V}(O)(bpy)_2]^{4+}$ as a kinetic transient, followed by rapid O-atom transfer to a water molecule to give the intermediate peroxide, $[(bpy)_2(O)Ru^{V}ORu^{III}(OOH)(bpy)_2]^{4+}$. The peroxide intermediate undergoes further oxidation and O_2 release, returning the complex to the

water oxidation cycle. Water oxidation catalysis by the blue dimer is inhibited by anion capture, which accompanies O_2 release.[2]
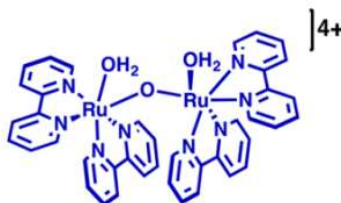
Figure 1.9 Structure of the Ruthenium "blue dimer" cis, cis-[(bpy)$_2$(H$_2$O)Ru^{III}ORu^{III}(OH$_2$)(bpy)$_2$]$^{4+}$. Courtesy: *Chem .Rev.*, **2015**, 115(23), pp.13006-13049.[4]

Ruthenium (Ru) polypyridyl chromophore and a Ru-based WOC were synthesized in 2014 by scientist Sun and co-workers. Their terminal positions were attached with phosphoric acid anchoring groups, carboxylic acid anchoring groups, respectively, as shown in Figure 1.9. Here, Ru-based water oxidation catalyst and Ru-based chromophore is linked by a bridging group Zirconium (Zr)(IV) –phosphate bridge (figure1.9 A) and phosphate–Zr-carboxylate bridge (figure 1.9 B) linkages to construct a "layer-by-layer "model (Ru-Zr^{4+}-Ru). This whole chromophore-catalyst system is functionalized with a phosphate anchoring group that can bind to the TiO$_2$ photoanode. [2,9,10]
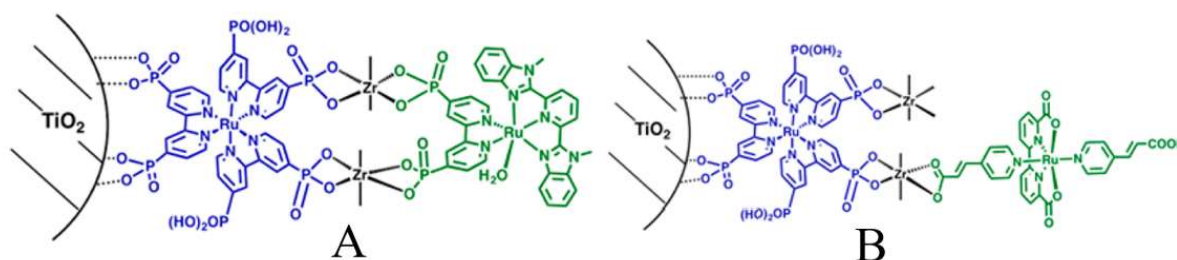
Figure 1.10. Example for co-valent linked chromophore catalyst system. (A) The "layer-by-layer" model of the dye (Ru-Zr^{4+}-Ru) connected to the catalyst by (A) Zirconium (IV) –phosphate bridge. Courtesy: Angew. Chem., Int. Ed. **2012**, 51, 12782− 12785. [16] (B) phosphate–Zr-carboxylate bridge. Both A and B are attached on TiO2 by the phosphoric acid anchoring group. Courtesy: *ACS Catal*. **2014**, 4, 2347−2350 [9]

In the given figure 1.11. they incorporated Iridium oxide nanoparticles as the WOC in photo anodes for DSPECs and provided the first example of DSPEC water splitting. In this design, the RuP^{2+}-like chromophore is derivatized with a malonate group for selective binding to the IrO$_x$

WOC. IrO_2 has been shown to be a rapid and efficient WOC that operates at relatively low overpotentials, making the Ru (II) polypyridyl chromophore−IrO_x an attractive candidate for the electrode design.
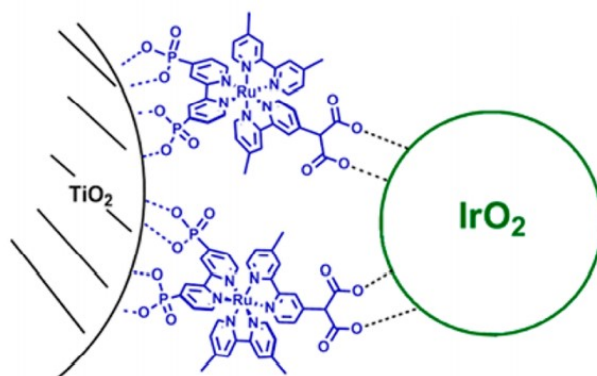
Figure 1.11. Example of a chromophore−oxide nanoparticle assemblies (Molecular-based assembly). This consists of a water oxidation catalyst that is linked to chromophore by a bridging ligand. This whole system is functionalized with semiconductor-metal oxide by an anchoring group. *Chem. Rev.*, **2015**, 115(23), pp.13006-13049. Reprinted with permission from ref 2. Copyright 2015 American Chemical Society.

1.7. Major challenges in this field:

- **Prevention of BET**: In multi chromophore–catalyst systems, the central chromophore should be well-engineered for rapid charge separation across the oxide interface. The distance between core antennas should be optimized through suitable spacers to prevent BET. Otherwise, back electron transfer will decrease the overall efficiency of any dye-sensitized photo electrochemical cell.

- **Stabilized surface binding and chemical stability**: The various surface anchoring groups must be chosen carefully for both the dye and catalyst molecules in order to prevent separation from the photoanode surface and successful transfer of the injected electrons. Carboxylic acid and phosphonic acid, two commonly used anchors, are observed to have poor stability in aqueous environments that result in the surface hydrolysis and dropping of catalytic function. [11]

- **Proper energy band gap engineering**: In multichromophoric systems, there must be a spectral overlap between the peripheral chromophore (donor) emission and central

chromophore (acceptor) absorption spectra for efficient FRET. Also, transition dipoles of donor emission and acceptor absorption should align favorably to facilitate the FRET to occur efficiently. However, designing such a multichromophoric system satisfying the optical and electronic properties to achieve multiple functions (light harvesting, electron transfer, anchoring, etc.) is challenging to achieve synthetically.

- **The strong tendency of PDIs to form π-π aggregates is a challenge**: Perylenediimide (PDI) has a strong tendency to form π-π aggregates; thus, the synthesis of perylene based light-harvesting antennae needs careful design. Long alkyl chains connected to these chromophores that can impart sufficient solubility and prevent undesirable aggregation are essential. Also, suitable non-conjugated spacers that can prevent electron transfer and its competition with the desired energy transfer process are highly desired.

- **Photostability of Chromophore:** Generally, organic chromophores undergo photobleaching (degradation of the π-framework) on light exposure (p); but perylene diimide is photochemical stable and thus desirable in the design of DSPEC type systems.

1.8. Possible questions to address:

1) **Metal free chromophores are rare:**

In most of the DSPECs till now, metalated chromophores have been used for photocatalytic studies, mainly Ru-based chromophores.[12] However, Ru metal is highly toxic as well as less eco-friendly. These metals are not economical as they are costly as compared to metal free chromophores. The latter could reduce the cost of designing DSPECs significantly.

2) **FRET based light-harvesting antenna in DSPECs are not explored yet:**

The maximum light of the solar spectrum can be harvested by designing the multichromophoric FRET cassettes that have complementary absorption spanning the wide range of the visible part in the solar spectrum, i.e., in the range of 400 to 700 nm. FRET based systems are expected to have many advantages like rapid exciton migration and prevention of back electron transfer, fast charge injection into the anode, and hole injection into the catalyst, which will help increase the overall efficiency of the DSPECs.

Therefore, we aim to explore the possible incorporation of FRET systems in the design of DSPEC systems.

1.9. Choice of energy donor and energy acceptor components to design chromophore catalyst systems according to two design strategies

1.9.1. Perylene (Energy acceptor)

Perylenes are a class of chromophore well-known for their exceptional photochemical stability, strong and broad absorption in the visible region, and synthetic versatility. Perylene-based antenna molecules carrying various donors have been reported, along with larger antenna systems in which perylenebisimides are intermediate energy donors. An unfavorable feature of PBI dyes is their high electron deficiency. Therefore PBI assemblies tend to undergo facile charge-separation when PBIs are coupled with even moderately electron-rich chromophores. One important structural feature of perylene is the presence of three different positions around the perylene core for substituents' attachment. Imide, bay (1, 6, 7, 12), and the ortho (2, 5, 8, 11) are the positions for the attachment of substituents. Figure 1.12 shows these three positions of the perylene core. The substitutions at bay position and imide position influence the optoelectronic and self-assembling properties of the dye.[20] Perylene can form good energy transfer pair with naphthalimide and several other chromophores such as anthracene and naphthalene diimide (NDI).[7]

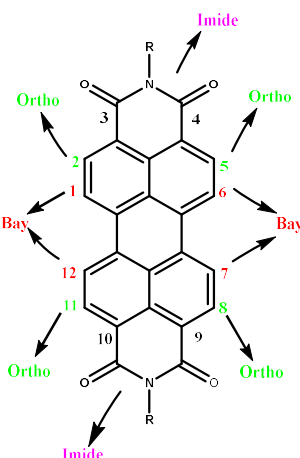
Figure 1.12. Chemical structure of PDI showing three different positions for substitution.

14

1.9.2. Naphthalimide (Energy donor)

Naphthalimide dyes possess great ease for modification and manipulation of their structure in order to tune their optoelectronic properties. As one of the classical fluorophores, naphthalimides have been widely used by various receptors due to their many excellent properties, such as good photostability, high fluorescence quantum yields, large Stokes' shifts.[14] These dyes are highly fluorescent, and their HOMO-LUMO energy levels and absorption profiles are complementary to those of PDI. Naphthalimide and PDI, therefore, form good FRET pairs.[15] The chemical structure of naphthalimide is shown in figure 1.13.
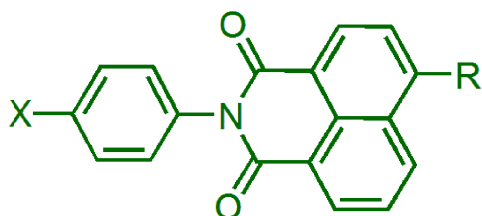
Figure 1.13. Chemical structure of naphthalimide.

1.9.3. Naphthalimide chromophore as energy donor and perylene as an energy acceptor

PDI was chosen as energy acceptor chromophore and naphthalimide as energy donor chromophore due to their complementarity in the absorption spectrum and good overlap of naphthalimide emission and perylene absorption as depicted in figure 1.14.[15]
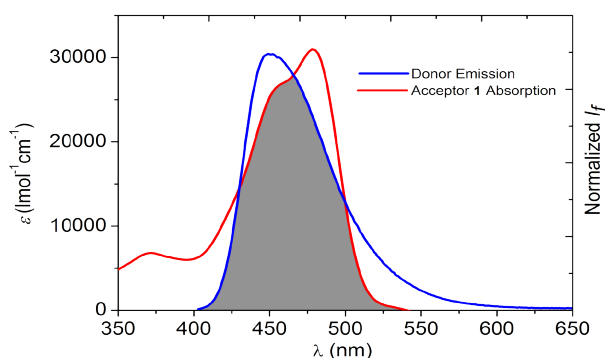
Figure 1.14. Spectral overlaps of emission of naphthalimide donor and absorption of perylene acceptor showing that they form a good FRET pair. Courtesy: *Chem Sci*, **2016**, 7, 3517-3532.[9]

1.10. Objective of the work

The main goal of this thesis was to synthesize a light-harvesting antenna synthetically functionalized with water oxidation catalyst (WOC) as well as a chromophore-catalyst assembly to achieve photocatalytic water oxidation into a more straightforward artificial photosynthesis system. Multiple chromophores capture light energy and transfer this energy into a central chromophore by a process called Forster resonance energy transfer (FRET). The judicious selection of energy donor chromophore and energy acceptor chromophore determines the light-harvesting antennae's energy transfer efficiency. For this work, perylene was chosen as energy acceptor chromophore and naphthalimide as energy donor chromophore due to their complementarity in the absorption spectrum. They form an excellent FRET pair, as known from the literature.[15] Thus, the aim here is to design robust and efficient organic chromophore-catalyst systems and assemblies for adsorption on photoanode using a modular synthetic approach in which multiple chromophores in a step-wise manner will be synthetically combined into a single molecule. We have designed two strategies for multichromophore catalyst system (figure 1.16)

- **Multichromophore catalyst co-loading system**: In the co-adsorption strategy, both chromophore and water oxidation catalysts are separately functionalized with anchoring groups for binding to the photoanode. We have termed the multichromophoric co-loading system as the SA-N-P-N (Surface anchoring group-naphthalimide-perylene-naphthalimide) system. The design and synthesis of the water oxidation catalyst functionalized with the anchoring group for photo anode binding are separately pursued in our group.

- **Covalently linked multichromophore-catalyst system:** In this design, chromophore, and water oxidation catalysts are covalently linked, and they are functionalized with anchoring groups for binding to the photoanode. We have termed the covalently linked multichromophore–catalyst system as the SA-N-P-N-Catalyst (Surface anchoring-naphthalimide-perylene-naphthalimide-catalyst) system
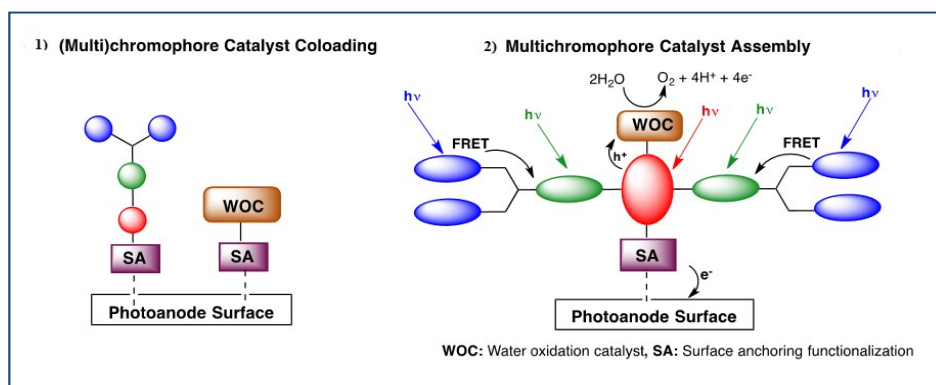
Figure 1.15. Schematic representation of molecular design: 1) Chromophore catalyst co-loading assembly involves surface anchoring functionalization of a single or multichromophores for binding to photoanode. 2) Multichromophore-catalyst system which consists of red, green, and blue chromophores and functionalized with water oxidation catalyst and surface anchoring group.

1.11. Compounds to be synthesized

1) **SA-N-P-N system:** This system consists of perylene (P) as energy acceptor, naphthalimide (N) as energy donor in bay position, and diisopropyl aniline in peri position of the perylene. Perylene can form good energy transfer pair with naphthalimide. In this system, there will be efficient energy transfer. The molecule at the other peri position is functionalized with an anhydride surface anchoring (SA) group. Therefore, we abbreviate this molecule as the SA-N-P-N system, as depicted in Figure 1.16.
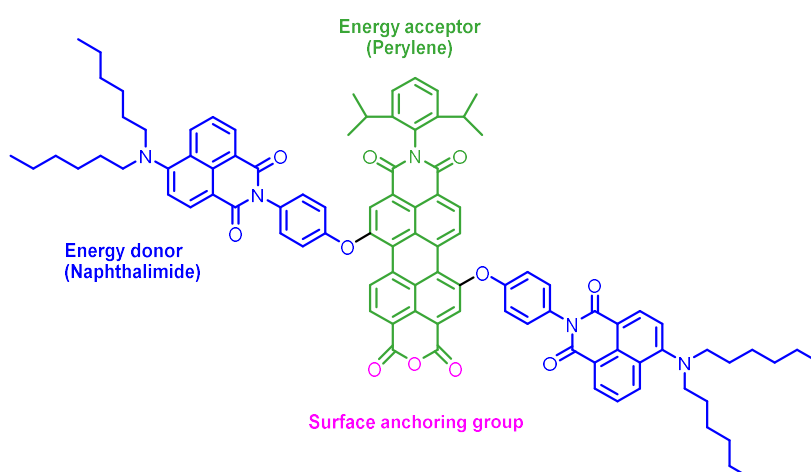

Figure 1.16. SA-N-P-N System consists of a surface anchoring group, naphthalimide as an energy donor, perylene diimide as an energy acceptor.

17

2) SA-N-P-N-Catalyst: This system consists of perylene (P) as energy acceptor, naphthalimide (N) as energy donor in bay position, and Iridium (Ir) based WOC (catalyst) in peri position of perylene. The Ir-based complexes containing pentamethylcyclopentadiene (Cp*) ligand and phenyl pyridine are highly active and robust WOCs, as reported by Crabtree, Brudvig, and co-workers.[14,17] The methyl spacer in the catalyst was introduced between central chromophore perylene and WOC to prevent the chances of charge recombination. The unsaturated first coordination sphere functions are the active site for the substrate water molecule, and catalyst allows the accumulation of multiple charges to form a high-valent metal-oxo intermediate which is essential for the water oxidation process.[18] The other peri position is functionalized with an anhydride surface anchoring (SA) group. Therefore, we abbreviate this molecule as SA-N-P-N-catalyst system, as depicted in figure1.17.
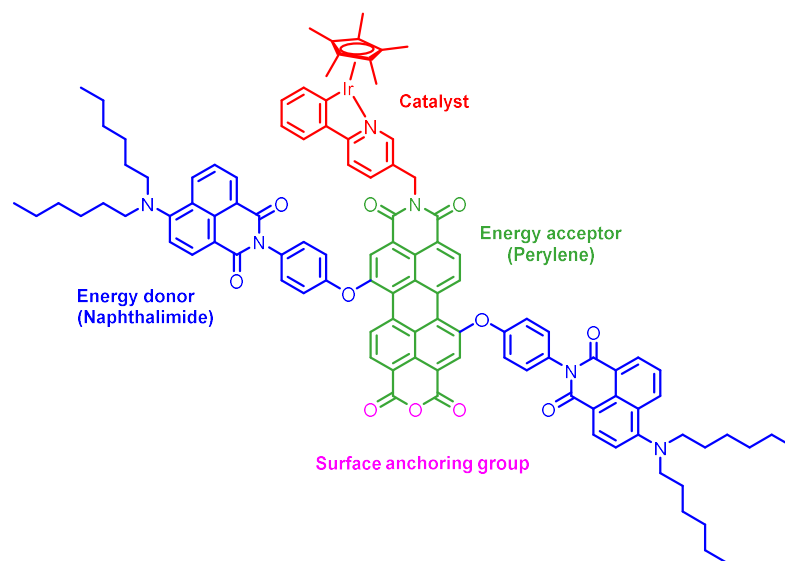

Figure 1.17. SA-N-P-N-catalyst system consists of a surface anchoring group, naphthalimide as an energy donor, perylene diimide as energy acceptor, and a water oxidation catalyst part.

18

Chapter 2

Results and discussion

As discussed in the introduction section (Chapter 1), this project intended to design and synthesize multichromophore-catalyst compounds according to the following two design strategies:

1) **Multichromophore catalyst co-loading system**: In co-adsorption strategy, both chromophore and water oxidation catalyst are separately functionalized by anchoring groups so that they can bind to the photoanode surface accordingly. We have termed such a system as the SA-N-P-N system.

2) **Covalently linked multichromophore catalyst system**: In this design, multichromophoric system will be synthesized first followed by covalent attachment of water oxidation catalyst to one end of the multichromophoric system and covalent attachment of the anchoring group at the other end of the multichromophoric system such that it can bind to the photoanode surface. We term such a system as SA-N-P-N-catalyst as discussed in chapter 1.

In both of the above design strategies, SA indicates the surface anchoring group, the anhydride terminus of the central chromophore, P indicates perylene central chromophore, an energy acceptor, and N indicates naphthalimide as the peripheral energy donor chromophore. The main intention of utilizing P and N in the multichromophoric system design is based on the fact that P and N form an efficient FRET pair with energy transfer efficiencies of 80-90% and ultrafast energy transfer from N to P in picoseconds timescale.[5] Furthermore, it is relatively straightforward to introduce an anhydride end in the perylene chromophore,. It has been shown that anhydride binds effectively to the TiO_2 photoanode [17] that we intend to use in our final artificial photosynthetic device design. Therefore, an anhydride functionality in our molecular design serves as the effective binding unit, i.e., surface anchoring group.[19]

Accordingly, we started the project with the synthesis of the naphthalimide subchromophore **(Scheme 1)** that serves as the energy donor unit of the multichromophore unit in both the design strategies.
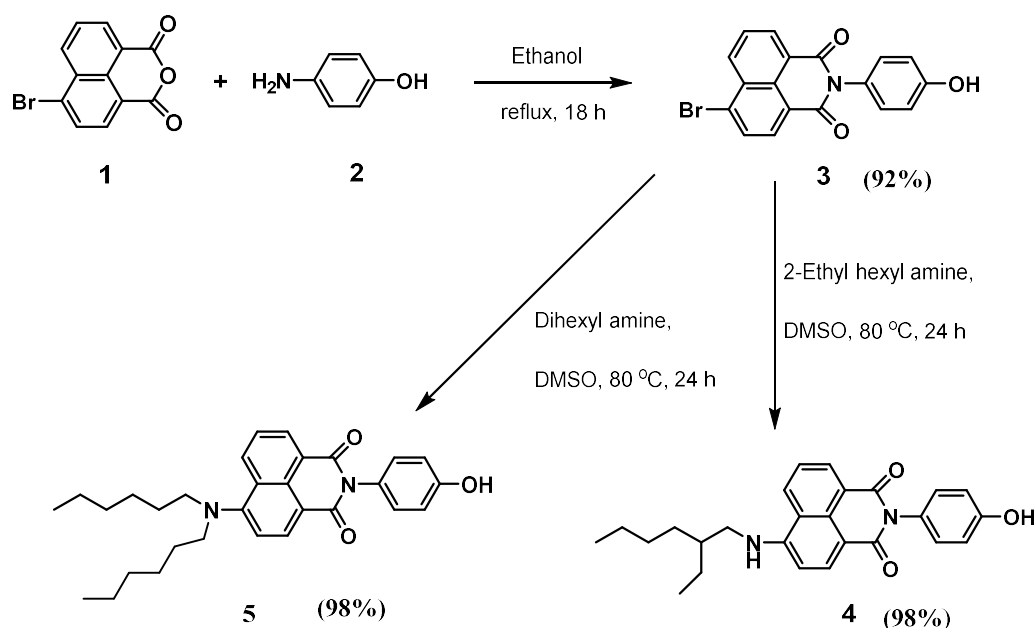
Scheme 2.1. Synthetic scheme of energy donor naphthalimide

Scheme 2.1. shows the two-steps synthetic route of energy donor naphthalimide where the first step is the amination of 4-bromo-1,8-naphthalic anhydride (**1**) with p-aminophenol, which is commercially available to obtain compound **3**. The first step was an 18-hour reaction with ethanol as the solvent used under reflux conditions. Subsequently, a simple substitution reaction of the bromo functionality was carried out to obtain compound **4,** where the Bromo group of **3** was substituted by 2-ethylhexylamine in the presence of dimethylsulphoxide (DMSO) as solvent and temperature of 80 ^{0}C for about 24 hours.

The NMR of the compound **4** was not pure, so we used a different aliphatic chain to attach it to the naphthalimide compound, i.e., dihexylchain chain. The substitution reaction of the Bromo functionality was carried out to obtain compound **5** where the Bromo group of 3 was substituted by dihexylamine in the presence of dimethylsulphoxide (DMSO) as solvent at a temperature of 80 ^{0}C for about 24 hours, followed by the synthesis of naphthalimide energy donor subchromophore, we proceeded with the synthesis of the perylene energy acceptor subchromophore as depicted in the scheme 2.2 below.
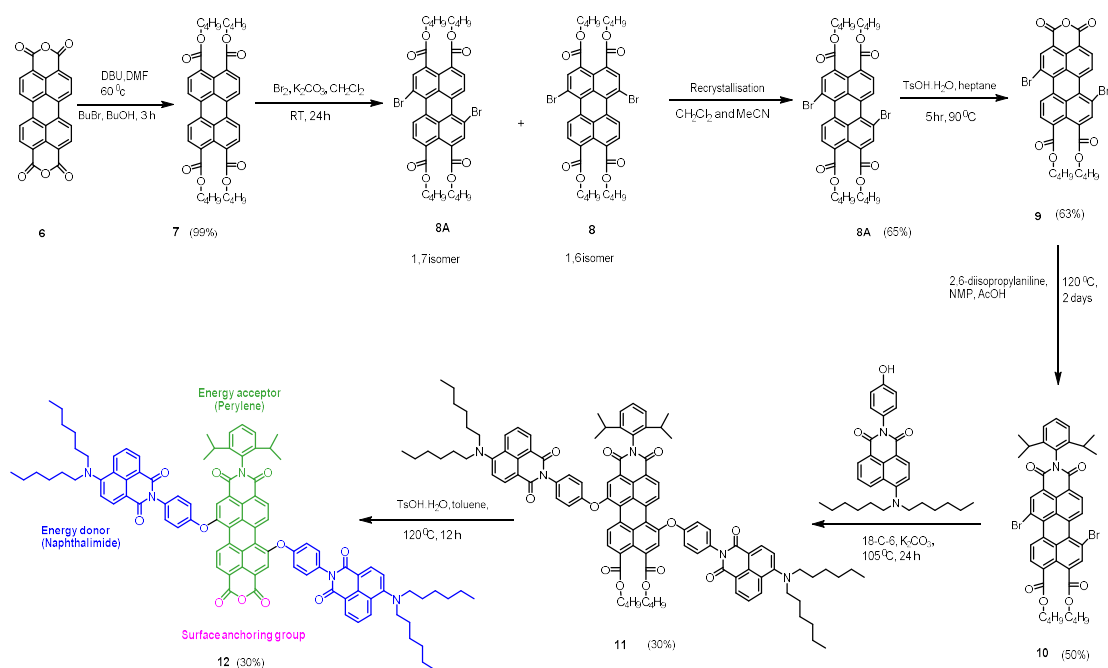
Scheme 2.2. Synthetic scheme of SA-N-P-N System

The synthetic scheme of the SA-N-P-N system is outlined in scheme 2.2. Starting with the commercially available perylene-3, 4,9,10 tetracarboxylic dianhydride. In the first step, perylene-3, 4, 9, 10-tetrabutylester (**7**) has been synthesized from compound **6** with high yield by opening up of the anhydride ring using reagents 1,8-Diazabicyclo[5.4.0]undec-7-ene (DBU) as a base and dimethylformamide (DMF) as solvent. The dibromination of compound 7 in DCM at room temperature was performed using Br_2 in the presence of K_2CO_3 as a base to obtain a mixture of 1, 7-isomer, and 1, 6-isomer. The desired compound was 1, 7 isomer (**8A**) that was achieved by the recrystallization from a mixture of two isomers (i.e., 1, 7- and 1, 6-isomers) using a solvent mixture of DCM and acetonitrile in a ratio of 1:9. After the crystallization, we were able to obtain a mixture 8A, and 8 in a ratio of 10:1.[20] After one more crystallization the pure 1, 7-isomer was achieved. The purification process was monitored by ^{1}H NMR spectroscopy. The conversion of compound **8A** to compound **9** (one ring closed perylene system, i.e., perylenemonoanhydride) was achieved by an acid-catalyzed (p-toluenesulphonic acid monohydrate) removal of two ester moieties in heptane as solvent at 90 °C for 5 hours. This

reaction also led to the formation of the bisanhydride side product (perlyenebisanhydride). Therefore, the mixture was again refluxed with methanol and a DCM washing was performed because the desired compound **8** (monoanhydride) was soluble in DCM while the side product (bisanhydride) was insoluble in DCM but soluble in methanol. Thus, based on the differential solubility of the monoanhydride and bisanhydride, the latter could be selectively removed, and the monoanhydride compound thus could be obtained in a pure form after DCM washing. The next step was the amination reaction of compound **9** that was performed with 2, 6-diisopropylaniline in N-methyl-2-pyrrolidone (NMP) as the solvent and acetic acid as catalyst. The reaction was kept at 120 ^{o}C for a duration of 2 days and the product formation was monitored by thin layer chromatography at regular intervals and finally, product was obtained by extraction (work up) method with DCM and water. Followed by the amination, we proceeded to attach the energy donor naphthalimide subchromophore at the bay positions of the perylene central chromophore. The attachment of naphthalimide (**5**) on bay position of perylene core was achieved by simple substitution of the 1,7-bromo substituents with the phenoxy functionalized naphthalimide subunits. The reaction was carried out in dry toluene at 90 ^{0}C in presence of K_2CO_3 as a mild base and 18-crown-6 as a phase transfer catalyst.[7] The desired compound was obtained in pure form after column chromatography and characterized by NMR spectroscopy. Compound **11** was to be further subjected to one-sided ring closure using p-toluenesulphonic acid monohydrate in presence of toluene as solvent to obtain compound **12** as and discussed earlier, the anhydride terminus of compound **12** (SA-N-P-N) will serve as the surface anchoring that will bind to the TiO_2 photoanode. In our group, further work is being carried out to design an Ir based water oxidation catalyst functionalized with surface anchoring group that can be used along with compound **12** for the co-adsorption studies as outlined in our molecular design strategy 1.[21] This system was successfully synthesized and UV/Vis absorption and fluorescence data was recorded.

Photophysical properties of synthesized compounds

The photophysical properties of all compounds were investigated by UV/Vis absorption and steady-state emission studies. UV/Vis absorption spectra of the reference subchromophores and antenna systems were recorded in chloroform at a concentration of ~ 10^{-5} M and are shown in figure 2.1.

Table 2.1. Absorption and emission wavelength of compound **5, 10, 11, 12.**

Compounds	λ_{abs} (nm)	λ_{em} (nm)	$\mathcal{E}$ (M^{-1} cm^{-1})
5	430	518	15 500
10	504	533	40 800
11	439	551	33,869
	506	554	37,478
12	435	554	4841
	529	560	8599

The energy donor naphthalimide **5** exhibited absorption at a shorter wavelength, i.e., 430 nm corresponding to the S_0-S_1 transition in naphthalimide, whereas the energy acceptor perylene **10** exhibited strong absorption λ_{max} at 504 nm. The molar extinction coefficient of the compound **5** and **10** are reported as 15,600 and 40,800 M^{-1} cm^{-1}, respectively in toluene.[15] A shoulder band was observed at 460 nm in the spectra of energy acceptor, a characteristic feature of perylene moieties.

The absorption spectra of the antenna system **12** clearly revealed the characteristic features of both donor and acceptor moieties (Figure 2.1). At shorter wavelengths, absorption is dominated by the naphthalimide chromophores (λ_{max} = 435 nm), whereas the absorption at longer wavelengths originates exclusively from the perylene chromophore (λ_{max} = 529 nm). Moreover, the spectra of the antennae system correspond to the sum of the spectra of constituents chromophores, indicating the absence of any ground-state interaction between them. However, there was a significant red-shift observed in the case of the ring closed antenna system **12** (~band at 530 nm) compared to the absorption maxima of **10** and **11** (at ~ 504/506 nm). Such red-shifted absorption could be attributed either to the chromophores' excitonic coupling or to the

23

aggregation of molecules of **12,** which upon ring-closing form closer π-π stacking with each other leading to the bathochromic shift.
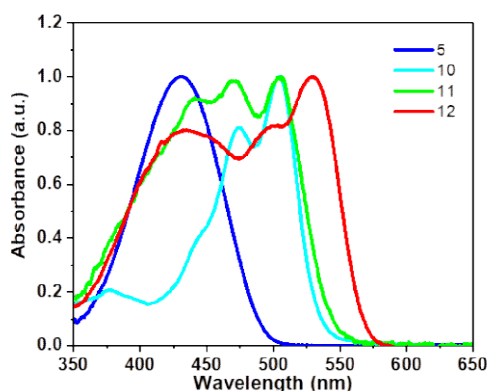

Figure 2.1. UV/Vis absorption spectra of energy donor **5,** energy acceptor **10,** the ring-open antenna system **11,** the ring-closed antenna system **12** in chloroform.

Steady-state fluorescence studies

Efficient transfer of excitation energy from the outer naphthalene chromophores to the inner perylene moiety is a prerequisite for a good light-harvesting antenna system that is to be employed in the design of an artificial photosynthetic system. Therefore, we first examined the spectral overlap between the donor **5** emission and acceptor **10** absorption**,** which is an important condition for efficient Förster resonance energy transfer. In the synthesized antenna system **12**, the donor's emission overlapped strongly with the absorption of acceptor moiety. For example, the donor compound **5** emits strongly in the range of 450-550 nm, and the acceptor compound **10** absorbs strongly in the same range, as shown in Figure 2.2
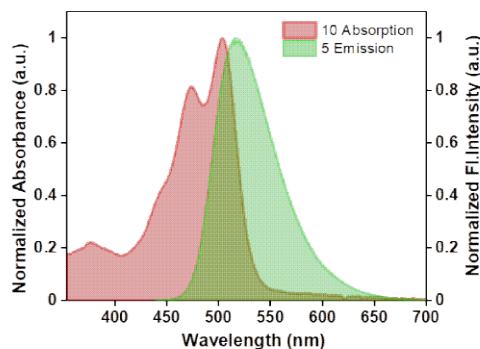
.

Figure. 2.2 Spectral overlap of the emission of donor molecule **5** with the absorption of acceptor molecule **10** in chloroform.

The energy acceptor was highly emissive fluorescence quantum yields of ca. 0.95 and singlet-state life-times around 4.6 ns[15] and was red-shifted compared to energy donor (Figure 2.3). The reference donor also exhibits strong emission ($\varphi_f > 0.75$) with singlet lifetimes in the range of 5.5–8.8 ns.[15] The fluorescence emission studies of the antenna molecule were performed at two separate wavelengths to achieve selective photoexcitation of only one of the chromophores.
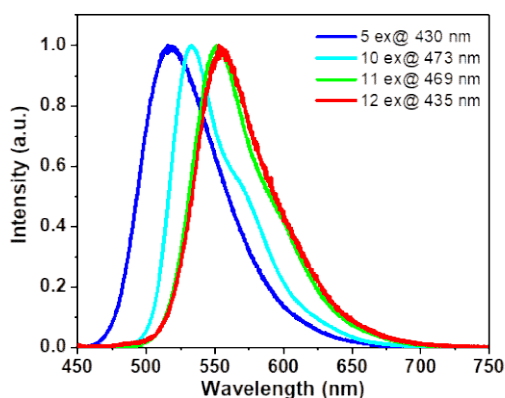

Figure 2.3. Normalized steady-state emission spectra of energy donor **(5)**, energy acceptor **(10)**, ring-open antenna system **(11)**, ring-closed antenna system **(12)** in chloroform.

Subsequently, the antenna molecules **11** and **12** were photoexcited at the absorption maxima of the naphthalimide **(5)** units, i.e., at 439 nm and 435 nm, respectively, but in the emission spectrum, there was no peak corresponding to donor emission, and high intensity peaks were obtained at 551 nm and 554 nm respectively for **11** and **12** corresponding to exclusive acceptor

emission. This observation indicates that energy transfer from energy donor to energy acceptor occurred upon photoexciting the antenna molecules (**11** and **12**) at the donor absorption bands. (Figure2.4.).
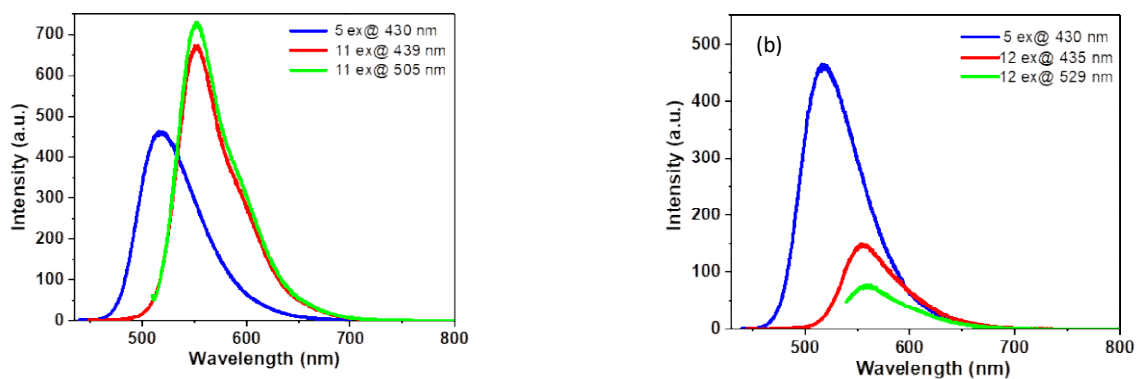

Figure 2.4. Steady-state emission spectra in chloroform of (a) energy donor (**5**)) λ_{ex} = 430 nm**,** ring-open antenna system (**11**) (a) 439 nm**,** ring-open antenna system (**11**)) λ_{ex} = 505 nm (b) energy donor (**5**)) λ_{ex} = 430 nm, ring-close antenna system (**12**)) λ_{ex} = 435 nm, ring-open antenna system (**12**)) λ_{ex} = 529 nm

Figure 2.5. shows the absorption of antenna molecule (12) with absorption maxima at 435 and 529 nm and emission in the range of 550-565 nm.
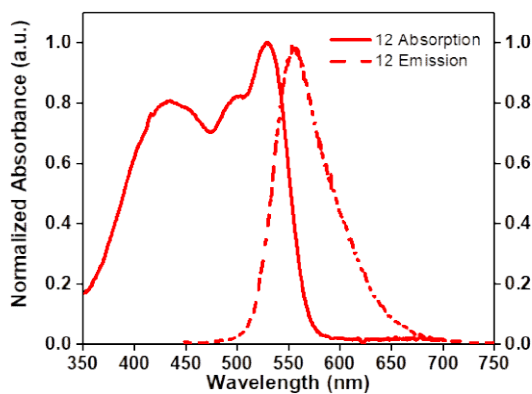
Figure 2.5. Emission spectrum of the ring-close antenna system **(12)** measured at $\lambda_{max} = 435$ nm (dashed line) along with the absorption spectrum (solid line) in chloroform

The fluorescence excitation spectra have a significant resemblance to the absorption spectra of the molecules **(11, 12),** which indicates efficient FRET occurring from naphthalimide to perylenes in both these compounds (ring open and ring closed) (Figure 2.6.).
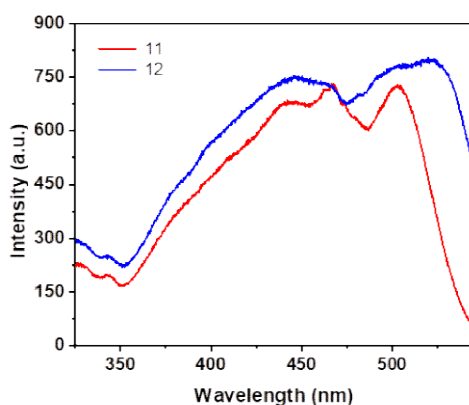
Figure 2.6. Fluorescence excitation spectrum of compound **11** and **12** measured at $\lambda = 551$ nm and 554 nm respectively recorded in chloroform.

Followed by photophysical investigation, in the future, the scope of this compound to adsorb it on TiO$_2$ photoanodes and Ir-based water oxidation catalyst precursor designed in our group will be pursued to obtain multichromophore-catalyst co-adsorption systems as discussed in the introduction Chapter 2.

Next, we proceeded with the synthesis of the SA-N-P-N-catalyst system according to design strategy 2 as depicted in the below scheme 2.3.
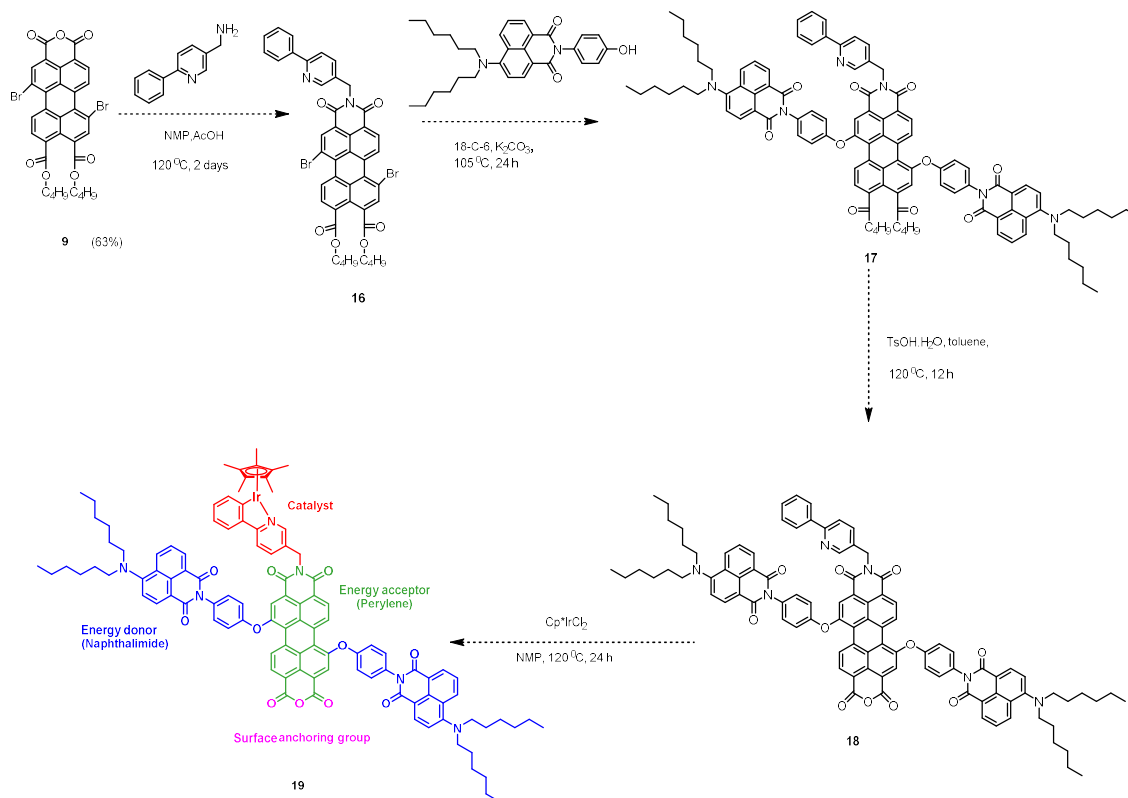
Scheme 2.3. Synthetic scheme of SA-N-P-N-Catalyst system

The synthetic scheme of the SA-N-P-N-catalyst system is outlined in scheme 2.3. We started the synthesis of the SA-N-P-N-catalyst system from compound **9**. The first step was the amination reaction of compound **9** with an amine-functionalized pyridine that will act as the precursor for attaching an Iridium water oxidation catalyst in the final step of the synthetic scheme. The amination reaction was performed with (6-phenylpyridin-3-yl)methanamine in NMP and acetic acid at 120 °C for a duration of 2 days. The (6-phenylpyridin-3-yl)methanamine was synthesized starting from 6-chloronicotinic acid that was subjected to thionyl chloride with toluene and aqueous ammonia for 8 h to give 6-chloronicotinamide. The 6-chloronicotinamide was subjected to Palladium-catalyzed Suzuki coupling with phenylboronic acid followed by reduction with sodium borohydride. **The dotted arrows are the synthesis work still remaining to be done in the project and will be pursued in the future· but the descriptions of the steps are summarized as follows**. The aminated compound **16** will be subjected to alkylation at 1,7-

positions with naphthalimide functionalized with phenol moieties in the presence of K_2CO_3 as base and 18-C-6 as the phase transfer catalyst to obtain the multichromophore–catalyst system **17**. Subsequently, **17** will be subjected to one-sided ring closure to obtain the monoanhydride compound **18**, where the anhydride functionality serves as the surface anchoring group for binding to the TiO_2 photoanode. Finally, compound **18** will be subjected to a reaction with $IrCpCl_2$, the water oxidation catalyst precursor in the presence of NMP as solvent at 120 ^{o}C for two days and the pyridine moiety in compound **18** chelates the Ir to finally give the product compound **19,** which will be the target compound SA-N-P-N-catalyst system. In all the above synthetic steps, purifications of the compounds were performed mostly by column chromatography and by recrystallization in one of the steps, and the correct structures were deduced by ^{1}H NMR spectroscopy as detailed in the experimental section (Chapter 4). The synthesis of this compound is going on with the preparation of the amine compound.

Chapter 3

Summary and Outlook

The objective of this thesis was to synthesize a multichromophoric system and assemblies for adsorption on photoanode in order to design an artificial photosynthetic device based on -dye-sensitized photo electrochemical cells. The main goal was to synthesize light-harvesting antennas and incorporate them into a simpler artificial photosynthetic system where multiple chromophores capture light energy and transfer this energy into a central chromophore that mimics a reaction center by a process called förster resonance energy transfer (FRET). The injection of the excited-state electron follows the absorption of light energy by chromophore into the semiconductor's conduction band, followed by transfer of the injected electron into the cathode with application of a bias to drive H_2 production. Intra-assembly electron transfer from the catalyst to chromophore will activate the catalyst toward the water oxidation and oxygen evolution at the water oxidation catalyst, followed by reduction of H_2O/H^+ to H_2 at the cathode

The judicious selection of energy donor chromophore and energy acceptor chromophore determines the energy transfer efficiency of light-harvesting antennae. For this work, perylene was chosen as energy acceptor chromophore and naphthalimide as energy donor chromophore due to their complementarity in the absorption spectrum, which we can clearly see from figure 2.2. and they form an excellent FRET pair as known from the literature.

We adopted two strategies for the design of the multichromophore-catalyst system (figure 1.16).

1. **Multichromophore catalyst co-loading system (SA-N-P-N)**: In the co-adsorption strategy, both chromophore and water oxidation catalysts are separately functionalized with anchoring groups for binding to the photoanode (See table 3.1). We have termed multichromophore co-loading system as the SA-N-P-N system where the chromophore will be functionalized with an anhydride anchoring group for binding to photoanode. The design and synthesis of Ir-based water oxidation catalyst functionalized with anchoring for photo anode binding are separately pursued in our group at present.

2. **Covalently linked multichromophore catalyst system (SA-N-P-N-catalys**t): In this design, chromophore and water oxidation catalysts are covalently linked, and they are functionalized with anchoring groups for binding to photoanode.

1. SA-N-P-N System   2. SA-N-P-N-Catalyst System
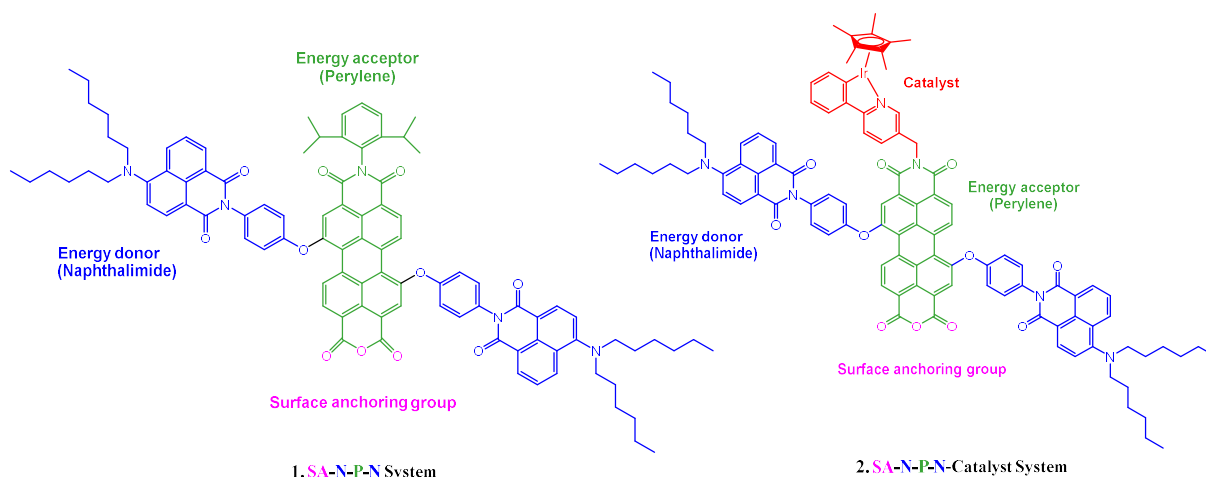
Energy donor and energy acceptor subchromophores have been successfully synthesized and characterized by ^{1}H NMR, ^{13}C NMR and the synthesis of the SA-N-P-N system was completed with complete structural characterization of the final compound. The remaining steps of SA-N-P-N-catalyst will be pursued in due course, and studies regarding their photophysical studies and eventual integration into an artificial photosynthetic device will be taken up.

Chapter 4

Experimental Section

General Information

4.1. Materials

All the chemicals and solvents were purchased from Sigma Aldrich, Merck and Himedia. Solvents like dichloromethane (DCM) were distilled using standard distillation setup. Toluene was dried by heating over sodium and using benzophenone as indicator. DCM was dried over phosphorus pentoxide and distilled prior to use. Column chromatography was carried out using silica gel of mesh size 60-120 as well as extraction of desired compounds after reaction were directly used without any further distillation. Reactions were monitored by checking thin layer chromatography (TLC) using TLC plates which were visualized under UV lamp (excitation wavelengths of 254 nm and 365 nm).

4.2. Methods

The ^{1}H NMR spectra were recorded on a 400 MHz Bruker Biospin Avance IIIFT-NMR and 500 MHz Avance Neo (Bruker) FT NMR spectrometer with TMS as standard at room temperature. CDCl$_3$ and DMSO-D$_6$ were the solvents used for doing NMR. Column chromatography was performed with silica gel of mesh size (60-120). UV-Vis was recorded on PerkinElmer LAMBDA 365 UV/Vis spectrophotometer, using a thermo stated quartz cuvette with 1 mm path length at 25 0 C. Fluorescence solution measurements were performed with Hitachi F7000 fluorescence spectrophotometer. The spectrometer was equipped with R928F photomultiplier expandable up to 900 nm. Standard software FL Solutions was used for the measurement and analysis of the data. Various excitation wavelengths were used to perform the fluorescence measurements.

4.3. Synthesis of donor precursor

4.2.1. Synthesis of N-(4-hydroxyphenyl)-4-bromonaphthalene-1, 8-dicarboxymonoimide
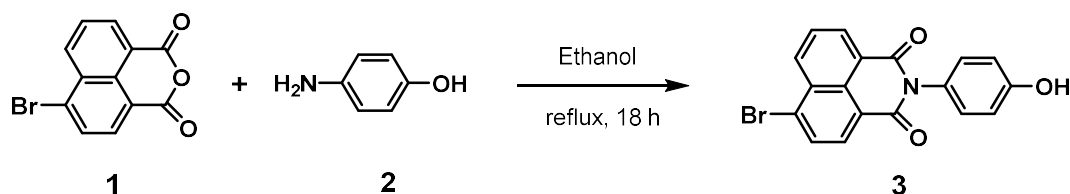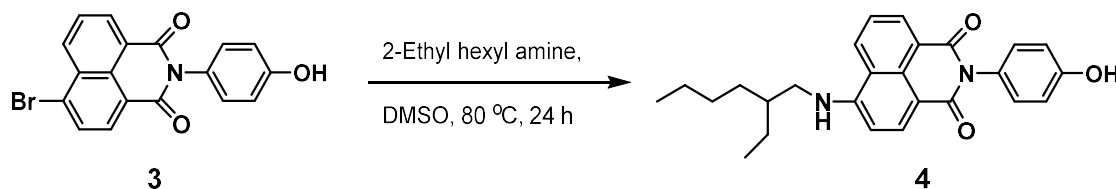

Scheme 4.1. Synthesis of N-(4-hydroxyphenyl)-4-bromonaphthalene-1, 8-dicarboxymonoimide.

A mixture of 4-bromo-1, 8-naphthalic anhydride (1 g, 3.61 mmol) and 4-aminophenol (0.4690 g, 4.30 mmol) in ethanol (40 mL) was refluxed for 18 hours (h). The reaction mixture was filtered after being cooled to room temperature. Subsequently, the residue was washed with ethanol and dried in vacuum oven to obtain compound **3** as an off-white solid compound with a yield of 92 %.

^{1}H NMR (400 MHz, DMSO-d$_6$):δ (ppm) = 9.69 (s, 1 H), 8.57 (t, J = 8 Hz, 2 H), 8.33 (d, J = 8 Hz, 1 H), 8.24 (d, J = 8 Hz, 1 H), 8.02 (t, J = 8 Hz, 1 H), 7.14 (d, J = 8 Hz, 2 H), 6.87 (d, J = 8 Hz, 2 H).

4.3.2. Synthesis of (4-hydroxyphenyl)-4-(ethylhexanamine)naphthalene-1, 8-dicarboxy monoimide
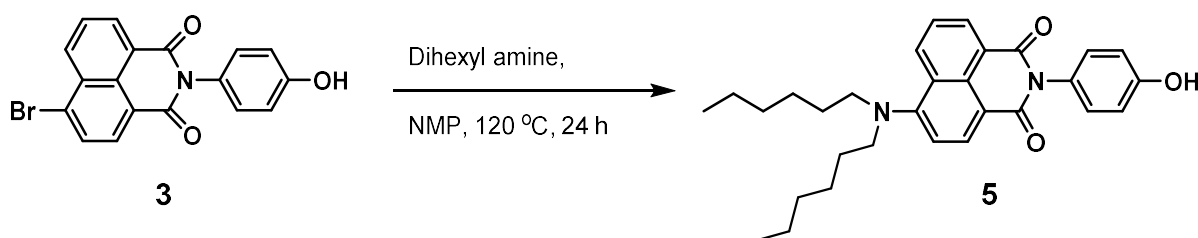

Scheme4.2. Synthesis of (4-hydroxyphenyl)-4-(ethylhexanamine)naphthalene-1, 8-dicarboxy monoimide.

N-(4-hydroxy phenyl)- 4-bromonaphthalene-1, 8-dicarboxy monoimide (852 mg, 2.32 mmol), ethyl hexane amine (4.472 g, 34.60 mmol) and DMSO (30 mL)were taken in a 50 mL round-bottomed (RB) flask. Subsequently, the reaction mixture was stirred at 80 °C for 24 h and the

resultant solution was poured in water (200 mL) to precipitate the crude product. But the precipitate was not formed, then extraction was performed using DCM and water, organic layer was passed through sodium sulphate and the solvent was removed using the rotary evaporator under vacuum and the solid was dried in a vacuum oven to obtain orange solid compound **4** with a yield of 98 %.

^{1}H NMR (400 MHz, DMSO): δ(ppm) = 9.60 (s, 1 H), 8.77 (d, J = 8.1 Hz, 1 H), 8.42 (d, J = 7.1 Hz, 1 H), 8.25 (d, J = 8.5 Hz, 1 H), 7.79 (t, J = 5.4 Hz, 1 H), 7.73 – 7.68 (m, 1 H), 7.05 (d, J = 8.7 Hz, 2 H), 6.84 (d, J = 8.7 Hz, 2 H), 3.29 (t, J = 6.2 Hz, 2 H), 1.81 (dd, J = 11.6, 5.7 Hz, 1 H), 1.42 – 1.27 (m, 8 H), 0.91 (t, J = 7.4 Hz, 3 H), 0.87 (t, J = 7.0 Hz, 3 H).

4.3.3. Synthesis of (4-hydroxyphenyl)-4-(dihexylamine)naphthalene-1, 8-dicarboxy monoimide

Scheme4.3. Synthesis of (4-hydroxyphenyl)-4-(dihexylamine)naphthalene-1, 8-dicarboxy monoimide.

N-(4-hydroxy phenyl)- 4-bromonaphthalene-1, 8-dicarboxy monoimide **1** (3 g, 8.15 mmol), dihexylamine (9.06 g, 48.88 mmol) and N-methyl-2-pyrrolidone (NMP) (30 mL) were taken in a two neck round-bottomed (RB) flask under nitrogen atmosphere and the reaction mixture was stirred at 120 °C for 24 h. After being cooled to room temperature, an aqueous solution of 10 % H_2SO_4 was added to the reaction mixture, and a gel-like mixture was formed which was filtered and then purified by silica gel column chromatography by eluting with hexane / ethyl acetate (3 / 1 v/v) and an yellow solid compound was obtained in 60 % yield.

^{1}H NMR (400 MHz, CDCl$_3$): $δ$ (ppm) = 8.63 (d, J = 8 Hz, 1 H), 8.53 (d, J = 8 Hz, 1 H), 8.48 (d, J = 8 Hz, 1H), 7.69 (t, J = 8 Hz, 1H), 7.22 (d, J = 8 Hz, 1H), 7.08 (d, J = 12 Hz, 2H), 6.83 (d, J = 8 Hz, 2H), 6.27 (s, 1H), 3.39 (t, J = 8 Hz, 4H), 1.65 - 1.58 (m, 4H), 1.31 - 1.26 (m, 12H).

^{13}C NMR (400 MHz, CDCl$_3$): δ (ppm) = 165.57, 165.10, 156.63, 156.36, 133.00, 131.89, 131.63, 130.88, 129.37, 127.35, 127.11, 125.23, 123.24, 116.94, 116.75, 115.04, 53.87, 31.66, 27.17, 26.94, 22.69, 14.12.

4.4. Synthesis of Acceptor Precursor

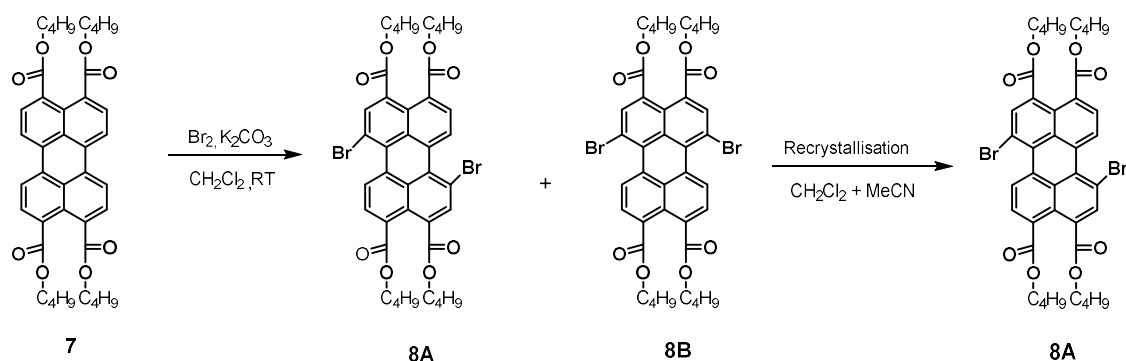### 4.4.1. Synthesis of perylene-tetracarboxylic tetrabutyl ester
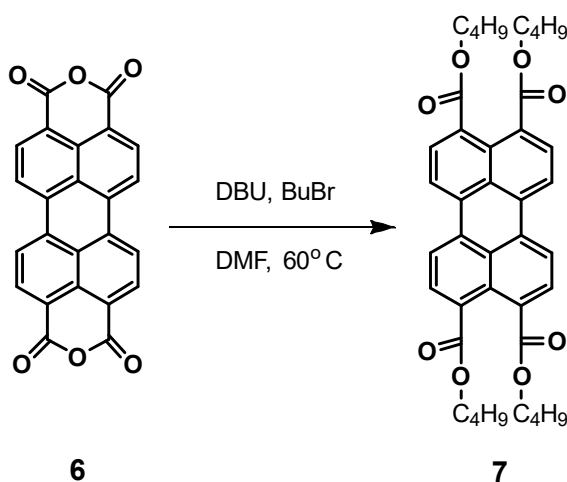
Scheme 4.4. Synthesis of perylene-tetracarboxylic tetrabutyl ester

A mixture of Perylene-3,4,9,10-tetracarboxylic dianhydride (PDA) (**6**) (500 mg, 1.26 mmol) , 1-8-Diazabicyclo[5.4.0]undec-7-ene (DBU) (767.3 mg, 0.753 mL), n-butanol (753.06 mg, 0.9 mL) was charged in 100 mL round-bottomed (RB) flask. Then, 6 mL DMF was added to RB and subjected to stirring for 0.5 h at 60 ^{0}C. Subsequently, 1-bromobutane (1.4 g, 0.0099 mmol) was added to the reaction mixture followed by the addition of another 5 mL of DMF and further kept stirring for 3 h. After cooling it down to the room temperature, the resulting solution was added to 100 mL of water and kept stirring for another 15 min, after which it was filtered. After the filtration process, the crude compound was subjected to the purification process by column chromatography on silica gel, eluting with DCM to obtain a golden orange solid compound with a yield of 91.6%.

^{1}H NMR (400 MHz, CDCl$_3$): δ (ppm) = 8.05 (d, J = 8 Hz, 4 H), 7.91 (d, J = 8 Hz, 4 H), 4.35 (t, J = 8 Hz, 8 H), 1.84-1.77 (m, 8 H), 1.55-1.48 (m, 8 H), 1.01 (t, J = 8 Hz, 12 H).

4.4.2. Synthesis of 1,7-dibromoperylene-3,4,9,10-tetracarboxyl tetrabutylester (3)
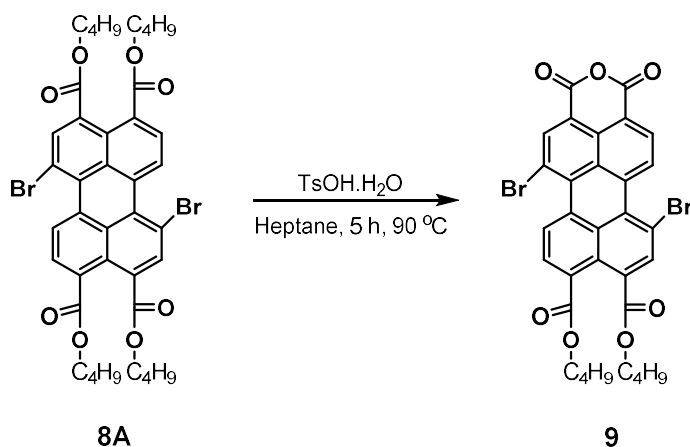

Scheme 4.5. Synthesis of 1,7-dibromoperylene-3,4,9,10-tetracarboxyl tetrabutylester

A mixture of perylene-tetracarboxylic tetrabutylester (**7**) (0.500 g, 0.766 mmol) and K_2CO_3 (0.250 g, 1.81 mmol) were taken into a 50 mL round-bottom flask, with a subsequent addition of CH_2Cl_2 (10 mL). Dropwise, bromine (0.500 mL, 9.70 mmol) was added to the resulting mixture and stirred for 24 h at room temperature. Afterward, an aqueous solution of sodium metabisulphite ($Na_2S_2O_5$) was added dropwise to the reaction mixture while stirring. The organic layer of the reaction mixture was washed with several portions of water and dried over sodium sulfate (Na_2SO_4). Followed by filtration, the solvent was removed by rotary evaporation to give the crude product (0.597 g) consisting of a mixture of 1,7- and 1,6-dibromo isomers. The isolation of the regioisomerically pure 1,7- isomer was accomplished by a double crystallization from dichloromethane/acetonitrile (1:9) solvent mixture. But the crystallization didn't take place because of some precipitate impurities. Therefore, column chromatography (DCM/ hexane) was carried for purification purposes in order to obtain the desired product. And then again, the crystallization step was done.

^{1}H NMR (400 MHz, CDCl3): δ (ppm) = 8.93 (d, J = 8 Hz, 2 H), 8.28 (s, 2 H), 8.08 (d, J = 8 Hz, 2 H), 4.34 (t, J = 8 Hz, 8 H), 1.78 (t, J = 8 Hz, 8 H), 1.51-1.46 (m, 8 H), 0.99 (t, J = 8 Hz, 12 H).

^{13}C NMR (400 MHz, CDCl3)): δ (ppm) = 168.02, 167.06, 136.67, 136.58, 133.51, 131.78, 131.72, 131.12, 130.42, 129.05, 127.63, 126.48, 118.72, 65.85, 65.63, 30.61, 30.58, 19.72, 19.24, 13.82.

4.4.3. Synthesis of 1,7-Dibromoperylene-3,4,9,10-tetracarboxy monoanhydride dibutylester
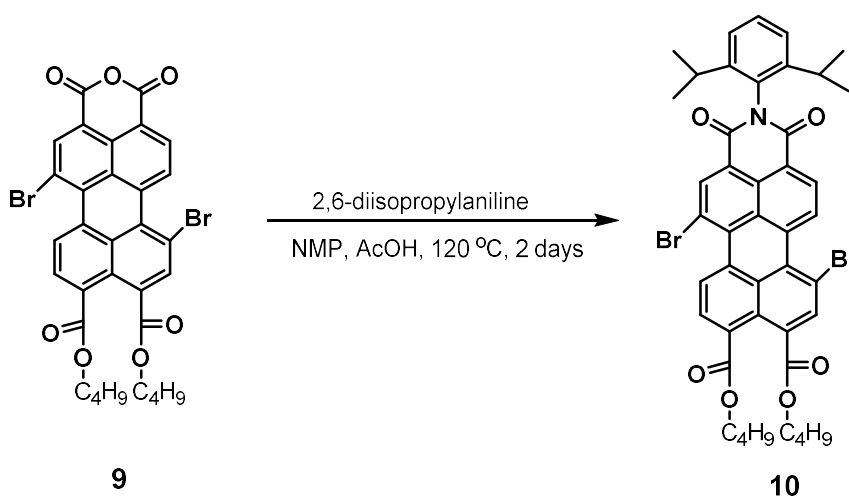

Scheme 4.6. Synthesis of 1,7-dibromoperylene-3,4,9,0-tetracarboxy monoanhydride dibutylester

Compound **8A** (200 mg, 0.25 mmol) and p-toluene sulfonic acid monohydrate (pTsOH·H$_2$O) (61 mg, 0.32 mmol) were taken in 50 mL round-bottomed (RB) flask and then 2 mL of heptane was subjected into the reaction mixture. Then the reaction mixture was stirred at 90 °C for 5 h. After some time, color change was noticed. The color of reaction mixture changed from orange to red with the formation of precipitate. After 5 h, the reaction mixture was allowed to cool to RT. Subsequently, the product was subjected to filtration and washed with small portion of water and methanol. Then the precipitate was dried in vacuum oven. This precipitate was taken in 100 mL methanol and kept for refluxing for another 3 h. Subsequently, reaction mixture was cooled to room temperature and subjected to filtration to remove the starting reagents. Then the residue was kept for drying and washed with small amount of DCM in order to remove the insoluble perylene bisimide side product. The solvent was evaporated by using rotary evaporator to get the desired compound. Then compound was subjected to silica gel column chromatography for purification of the desired compound first with DCM/hexane (1:1) then with pure DCM to obtain red solid compound **8** with a yield of 63 %.

^{1}H NMR (400 MHz, CDCl3): δ (ppm) = 9.30-9.24 (m, 2 H), 8.90 (s, 1 H), 8.68 (d, *J* = 8 Hz, 1 H), 8.35 (s, 1 H), 8.16 (d, *J* = 8 Hz, 1 H), 4.38-4.34 (m, 4 H), 1.84-1.76 (m, 4 H), 1.53-1.47 (m, 4 H), 1.03-0.98 (m, 6 H).

^{13}C NMR (400 MHz, CDCl$_3$): δ (ppm) = 167.74, 166.87, 162.49, 159.63, 159.31, 139.81, 132.62, 132.29, 132.20, 132.20, 130.09, 129.17, 129.08, 128.74, 128.42, 121.26,119.41, 118.06, 117.96, 102.29, 66.28, 66.28, 66.06, 30.70, 30.70, 30.67, 30.67, 29.84, 19.52, 19.34, 19.34, 19.03, 19.03.

4.4.4. Synthesis of N-(2,6-Diisopropylphenyl)-1,7-dibromoperylene- 3,4,9,10- tetracarboxy monoimide dibutylester
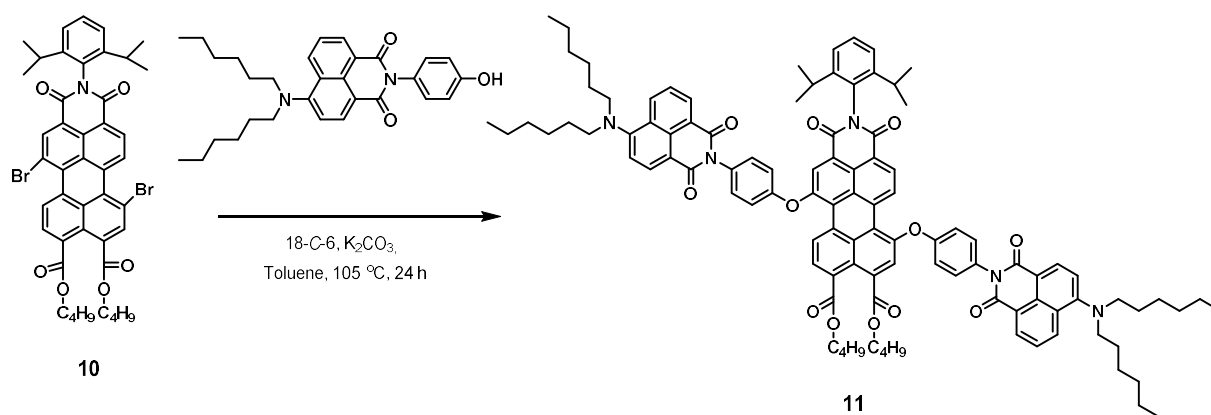

Scheme 4.7. Synthesis of N-(2,6-diisopropylphenyl)-1,7-dibromoperylene-3,4,9,10-tetracarboxy monoimide dibutylester

Dibromo perylene dibutylester monoanhydride (**9**) (50 mg, 0.73 mmol) was taken in a 100 mL RB flask and added 2,6-diisopropylaniline (28.7 mg, 1.58 mmol), acetic acid (0.023 mL, 0.40 mmol) and NMP (5 mL) into the RB flask. Subsequently, reaction mixture was stirred for two days at 120 °C under nitrogen atmosphere. The reaction mixture was kept at RT. After it reached room temperature, the reaction mixture was added into distilled water to obtain the precipitate. Then the remaining NMP was removed by washing precipitate with large amount of water. The same reaction was performed using 110 mg of the starting compound. But in this reaction precipitate was not formed when reaction mixture was poured to water. So, extraction was performed using DCM and water and the organic layers were dried over sodium sulphate and the solvent was evaporated using rotary evaporator under vacuum. Subsequently, the crude product was subjected for purification by column chromatography using DCM as eluent to obtain purple solid compound **9** with a yield of 50 %.

¹H NMR (400 MHz, CDCl3):δ (ppm) = 9.28 (d, J = 8 Hz, 1 H), 9.24 (d, J = 8 Hz, 1 H), 8.95 (s, 1 H), 8.73 (d, J = 8 Hz, 1 H), 8.28 (s, 1 H), 8.16 (d, J = 8 Hz, 1 H), 7.51 (t, J= 8 Hz, 1 H), 7.36 (d, J= 8 Hz, 2 H), 4.37 (t, J= 8 Hz, 4 H), 2.76-2.71 (m, 2 H), 1.83-1.77 (m, 4 H), 1.54-1.48 (m, 4 H), 1.18 (d, J= 6.7 Hz, 12 H) 1.01 (d, J = 8 Hz, 6 H).

4.4.5. Synthesis of (2,6-diisopropylphenyl)-1,7-bis[N-(pphenyloxy)-(4-(2-ethylhexanamine)-1,8-dicarboxynapthalenemonoimide)]perylene-3,4,9,10-tetracarboxymonoimidedibutylester
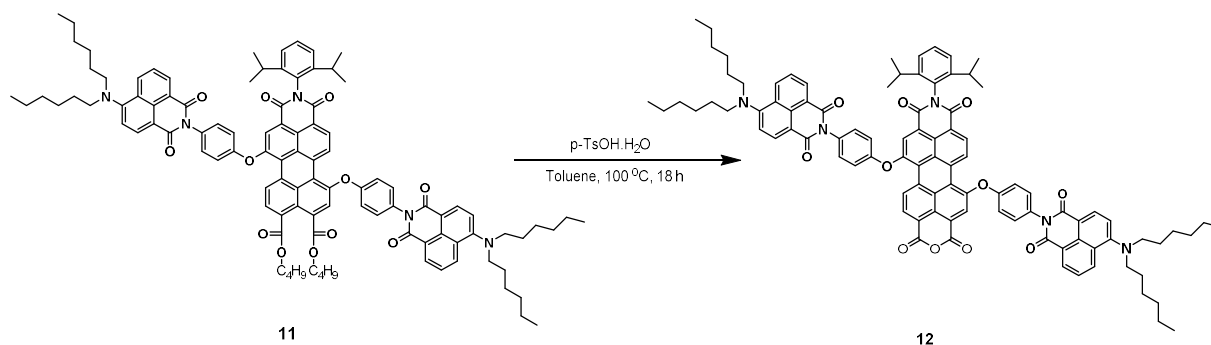

Scheme 4.8. Synthesis of (2,6-diisopropylphenyl)-1,7-bis[N-(pphenyloxy)-(4-(2-ethyl hexanamine)-1,8-dicarboxy napthalenemonoimide)]perylene-3,4,9,10-tetracarboxy monoimidedibutylester.

Compound **5** (80 mg, 0.17 mmol) was taken in a 50 mL RB flask and K₂CO₃ (48.5 mg, 0.351 mmol) and 18-crown-6 (121 mg, 0.46 mmol) were added into the RB flask followed by addition of 20 mL of dry toluene into the reaction mixture. The reaction mixture was stirred at room temperature for 30 minutes. Temperature was increased up to 50 °C so that compound **5** was completely mixed with toluene and then subsequently, compound **10** (45 mg, 0.054mmol) was added to the reaction mixture and temperature was increased to 105 °C. After 24 h, the reaction mixture was cooled down to room temperature and toluene was removed using rotary evaporation. Extraction was performed using DCM and water, the combined layers were dried over sodium sulphate and solvent was dried using rotary evaporator. The desired product was obtained by column chromatography using DCM/Hexane (7/3) as eluent for purification with an yield of 30 %.

1H NMR (400 MHz, CD₂Cl₂) δ (ppm) : 9.50 (d, *J* = 8.3 Hz, 1 H), 9.45 (d, *J* = 8.2 Hz, 1 H), 8.67 (d, *J* = 8.2 Hz, 1 H), 8.54 (d, *J* = 7.1 Hz, 2 H), 8.50 (s, 2 H), 8.47 (s, 1 H), 8.44 (d, *J* = 8.1 Hz, 2 H), 8.14 (d, *J* = 8.2 Hz, 1 H), 7.97 (s, 1 H), 7.67 (t, *J* = 7.6 Hz, 2 H), 7.49 (t, *J* = 7.7 Hz, 1 H),7.35-7.21 - (m, , 12 H), 4.34-4.27- (m, , 4 H), 3.38 (t, *J* = 6.7 Hz, 8 H), 2.78-2.72- (m, , 2 H), 1.82-1.71- (mm,), 1.59 (q, *J* = 7.2 Hz, 12 H), 1.60- – 1.28 (m, 16 H), 1.13 (d *J* = 4 Hz 14 H), 1.012– 0.94 (m, 8 H), 0.83 (q, *J* = 8.6, 6.8 Hz, 18 H).

¹³C NMR (400 MHz, CDCl₃) δ (ppm) : 168.05, 167.28, 164.66, 164.04, 163.06, 156.17, 155.60, 155.46, 152.79, 152.59, 146.13, 134.08, 133.32, 132.23, 132.03, 132.00, 131.47, 131.45, 131.42, 131.15, 131.13, 130.83, 130.78, 130.70, 130.65, 129.56, 129.45, 128.65, 128.11, 127.07, 126.45, 126.37, 125.26, 124.97, 124.02, 123.31, 123.20, 121.65, 118.65, 118.42, 116.53, 114.94, 114.91, 65.78, 65.50, 31.93, 31.55, 30.64, 30.49, 30.04, 29.70, 29.37, 29.07, 27.05, 26.79, 23.79, 23.73, 22.70, 22.58, 19.29, 19.22, 13.89, 13.75, 13.59.

4.4.5. Synthesis of (2,6-diisopropylphenyl)-1,7-bis[N-(pphenyloxy)-(4-(2-ethylhexanamine)-1,8-dicarboxynapthalenemonoimide)]perylene-3,4,9,10-tetracarboxymonoimidedibutylester

Scheme 4.9. Synthesis of (2,6-diisopropylphenyl)-1,7-bis[N-(pphenyloxy)-(4-(2-ethyl hexanamine)-1,8-dicarboxy napthalenemonoimide)]perylene-3,4,9,10-tetracarboxy monoimidedibutylester.

Compound **11** (20 mg, 0.012 mmol) and p-toluene sulfonic acid monohydrate (pTsOH·H₂O) (12 mg, 0.06 mmol) were taken in 25 mL round-bottomed (RB) flask and then 2 mL of toluene was subjected into the reaction mixture. Then the reaction mixture was stirred at 100 °C for 18 h.

After some time, color change was noticed. The color of the reaction mixture changed from orange to red with the formation of precipitate. After 18 h, the reaction mixture was allowed for cooling to RT. Subsequently, the solvent was evaporated and the residue was dissolved in $CHCl_3$. The organic phase was collected, dried over sodium sulphate (Na_2SO_4), and evaporated. Thereafter, MeOH (75 mL) was added to the solid residue and refluxed for 2 h. After cooling down to room temperature, the precipitate was collected by filtration, dried, and dissolved in minimum amount of refluxing $CHCl_3$. To this solution, MeOH was added to obtain the precipitateof the product. The blackish red precipitate was collected by filtration and dried to afford the pure product with a yield of 30 %.

^{1}H NMR (400 MHz, CDCl$_3$): δ(ppm) = 9.68 (d, J = 8.3 Hz, 1 H), 9.64 (d, J = 8.4 Hz, 1 H), 8.76 (d, J = 8.3 Hz, 1 H), 8.71 (d, J = 8.3 Hz, 1 H), 8.64 – 8.61 (m, 2 H), 8.58 (s, 1 H), 8.53 – 8.51 (m, 2 H), 8.49 (s, 1 H), 8.47 (d, J = 2.5 Hz, 1 H), 7.71-7.69 (m, , 2 H), 7.48 (d, J = 7.7 Hz, 1 H), 7.43 – 7.38 (m, 4 H), 7.36 – 7.29 (m, 6 H), 7.22 (dd, J = 4 Hz, 2 H), 3.38 (td, J = 7.6, 2.1 Hz, 6 H), 2.79 – 2.71 (m, 2 H), 1.60 (dd, J = 6.3, 4.3 Hz, 12 H), 1.42 – 1.35 (m, 2 H), 1.31-1.25 (m, 20 H), J = 1.5 Hz, 18 H), 1.18 (dd, J = 6.8, 4.0 Hz, 10 H), 0.84 (dd, J = 6.8, 5.6 Hz, 12 H).

4.5. Synthesis of amine precursor
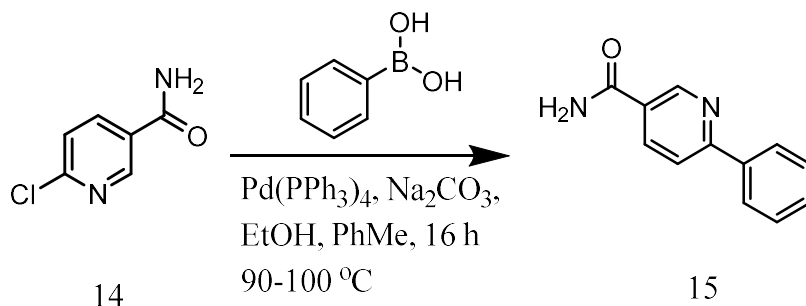### 4.5.1 Synthesis of 6-chloronicotinamide
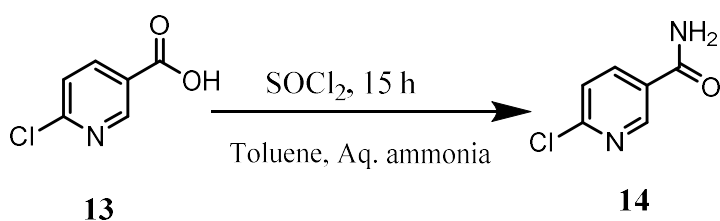
Scheme 4.10. Synthesis of 6-chloronicotinamide.

A mixture of **13** (1 g, 6.35 mmol) and distilled thionyl chloride (1.13 g, 9.52mmol) was refluxed for 15 h, and evaporated in vacuo to dryness. The residue was dissolved in toluene (4 mL). Subsequently the reaction mixture was stirred at room temperature for 8 h and filtered to give a white solid. The white solid was then dissolved in ethanol and then recrystallized to obtain colourless crystalline solid **13**. Yield: 30 %, m.p. 211-213 °C.

¹H NMR (400 MHz, DMSO) *δ* (ppm): 8.85 (d, *J* = 2.3 Hz, 1 H), 8.25 (dd, *J* = 8.3, 2.5 Hz, 1 H), 8.22 (s, 1 H), 7.71 (s, 1 H), 7.64 (d, *J* = 8.3 Hz, 1 H).

4.5.2. Synthesis of (6-phenylpyridine-3-yl)methanamine

Scheme 4.11. Synthesis of (6-phenylpyridine-3-yl)methanamine.

A mixture of 6-chloronicotinamide (14) (55 mg, 0.351 mmol), phenylboronic acid (47 mg, 0.386 mmol), and Pd(PPh$_3$)$_4$ (12.2 mg, 0.01 mmol) in toluene (4 mL), ethanol (4 mL) and 2M aqueous sodium carbonate solution (2 mL, 0.796 mmol) was stirred and heated at 90-100 °C under nitrogen for 16 h. The mixture was cooled to room temperature and filtered. The resulting solid was washed with water (2 × 20 mL) and dried in vacuo. To the dried solid was added methanol (50 mL). The mixture was stirred at reflux, cooled to room temperature, and filtered to give the product. Powder, yield 90 %. mp 218-220 °C;

Purification of this step was going on. So, nmr was not recorded.

References

(1)   Dau, H.; Zaharieva, I. Principles, Efficiency, and Blueprint Character of Solar-Energy Conversion in Photosynthetic Water Oxidation. *Acc. Chem. Res.* **2009**, *42* (12), 1861–1870. https://doi.org/10.1021/ar900225y.

(2)   Ashford, D. L.; Gish, M. K.; Vannucci, A. K.; Brennaman, M. K.; Templeton, J. L.; Papanikolas, J. M.; Meyer, T. J. Molecular Chromophore-Catalyst Assemblies for Solar Fuel Applications. *Chem. Rev.* **2015**, *115* (23), 13006–13049. https://doi.org/10.1021/acs.chemrev.5b00229.

(3)   Tachibana, Y.; Vayssieres, L.; Durrant, J. R. Artificial Photosynthesis for Solar Water-Splitting. *Nat. Photonics* **2012**, *6* (8), 511–518. https://doi.org/10.1038/nphoton.2012.175.

(4)   Kärkäs, M. D.; Verho, O.; Johnston, E. V.; Åkermark, B. Artificial Photosynthesis: Molecular Systems for Catalytic Water Oxidation. *Chem. Rev.* **2014**, *114* (24), 11863–12001. https://doi.org/10.1021/cr400572f.

(5)   Xia, X.; Song, M.; Wang, H.; Zhang, X.; Sui, N.; Zhang, Q.; Colvin, V. L.; Yu, W. W. Latest Progress in Constructing Solid-State Z Scheme Photocatalysts for Water Splitting. *Nanoscale* **2019**, *11* (23), 11071–11082. https://doi.org/10.1039/c9nr03218e.

(6)   Duonghong, D.; Borgarello, E.; Grätzel, M. Dynamics of Light-Induced Water Cleavage in Colloidal Systems. *J. Am. Chem. Soc.* **1981**, *103* (16), 4685–4690. https://doi.org/10.1021/ja00406a004.

(7)   Sengupta, S.; Dubey, R. K.; Hoek, R. W. M.; Van Eeden, S. P. P.; Gunbasç, D. D.; Grozema, F. C.; Sudhölter, E. J. R.; Jager, W. F. Synthesis of Regioisomerically Pure 1,7-Dibromoperylene-3,4,9,10- Tetracarboxylic Acid Derivatives. *J. Org. Chem.* **2014**, *79* (14), 6655–6662. https://doi.org/10.1021/jo501180a.

(8)   Suryani, O.; Higashino, Y.; Mulyana, J. Y.; Kaneko, M.; Hoshi, T.; Shigaki, K.; Kubo, Y. A Near-Infrared Organic Photosensitizer for Use in Dye-Sensitized Photoelectrochemical Water Splitting. *Chem. Commun.* **2017**, *53* (50), 6784–6787. https://doi.org/10.1039/c7cc02730c.

(9)   Youngblood, W. J.; Anna Lee, S. H.; Maeda, K.; Mallouk, T. E. Visible Light Water Splitting Using Dye-Sensitized Oxide Semiconductors. *Acc. Chem. Res.* **2009**, *42* (12), 1966–1973. https://doi.org/10.1021/ar9002398.

(10)   Bettis, S. E.; Hanson, K.; Wang, L.; Gish, M. K.; Concepcion, J. J.; Fang, Z.; Meyer, T. J.; Papanikolas, J. M. Photophysical Characterization of a Chromophore/Water Oxidation Catalyst Containing a Layer-by-Layer Assembly on Nanocrystalline TiO2 Using Ultrafast Spectroscopy. *J. Phys. Chem. A* **2014**, *118* (45), 10301–10308. https://doi.org/10.1021/jp411139j.

(11)   Wang, D.; Wang, L.; Brady, M. D.; Dares, C. J.; Meyer, G. J.; Meyer, T. J.; Concepcion, J. J. Self-Assembled Chromophore-Catalyst Bilayer for Water Oxidation in a Dye-Sensitized Photoelectrosynthesis Cell. *J. Phys. Chem. C* **2019**, *123* (50), 30039–30045. https://doi.org/10.1021/acs.jpcc.9b07125.

(12)   Song, W.; Ito, A.; Binstead, R. A.; Hanson, K.; Luo, H.; Brennaman, M. K.; Concepcion, J. J.; Meyer, T. J. Accumulation of Multiple Oxidative Equivalents at a Single Site by Cross-Surface Electron Transfer on TiO2. *J. Am. Chem. Soc.* **2013**, *135* (31), 11587–11594. https://doi.org/10.1021/ja4032538.

(13)   Dubey, R. K.; Eustace, S. J.; Van Mullem, J. S.; Sudhölter, E. J. R.; Grozema, F. C.; Jager, W. F. Perylene Bisimide Dyes with up to Five Independently Introduced Substituents: Controlling the Functionalization Pattern and Photophysical Properties Using Regiospecific Bay Substitution. *J. Org. Chem.* **2019**, *84* (15), 9532–9547. https://doi.org/10.1021/acs.joc.9b01131.

(14)   Blakemore, J. D.; Schley, N. D.; Balcells, D.; Hull, J. F.; Olack, G. W.; Incarvito, C. D.; Eisenstein, O.; Brudvig, G. W.; Crabtree, R. H. Half-Sandwich Iridium Complexes for Homogeneous Water-Oxidation Catalysis. *J. Am. Chem. Soc.* **2010**, *132* (45), 16017–16029. https://doi.org/10.1021/ja104775j.

(15)   Dubey, R. K.; Inan, D.; Sengupta, S.; Sudhölter, E. J. R.; Grozema, F. C.; Jager, W. F. Tunable and Highly Efficient Light-Harvesting Antenna Systems Based on 1,7-Perylene-3,4,9,10-Tetracarboxylic Acid Derivatives. *Chem. Sci.* **2016**, *7* (6), 3517–3532. https://doi.org/10.1039/c6sc00386a.

(16)   Duke, R. M.; Veale, E. B.; Pfeffer, F. M.; Kruger, P. E.; Gunnlaugsson, T. Colorimetric and Fluorescent Anion Sensors: An Overview of Recent Developments in the Use of 1,8-Naphthalimide-Based Chemosensors. *Chem. Soc. Rev.* **2010**, *39* (10), 3936–3953. https://doi.org/10.1039/b910560n.

(17)   Hull, J. F.; Balcells, D.; Blakemore, J. D.; Incarvito, C. D.; Eisenstein, O.; Brudvig, G.

W.; Crabtree, R. H. Highly Active and Robust Cp* Iridium Complexes for Catalytic Water Oxidation. *J. Am. Chem. Soc.* **2009**, *131* (25), 8730–8731. https://doi.org/10.1021/ja901270f.

(18) Zhang, B.; Sun, L. Artificial Photosynthesis: Opportunities and Challenges of Molecular Catalysts. *Chem. Soc. Rev.* **2019**, *48* (7), 2216–2264. https://doi.org/10.1039/c8cs00897c.

(19) Vagnini, M. T.; Smeigh, A. L.; Blakemore, J. D.; Eaton, S. W.; Schley, N. D.; D'Souza, F.; Crabtree, R. H.; Brudvig, G. W.; Co, D. T.; Wasielewski, M. R. Ultrafast Photodriven Intramolecular Electron Transfer from an Iridium-Based Water-Oxidation Catalyst to Perylene Diimide Derivatives. *Proc. Natl. Acad. Sci. U. S. A.* **2012**, *109* (39), 15651–15656. https://doi.org/10.1073/pnas.1202075109.

(20) Webb, J. E. A.; Chen, K.; Prasad, S. K. K.; Wojciechowski, J. P.; Falber, A.; Thordarson, P.; Hodgkiss, J. M. Quantifying Highly Efficient Incoherent Energy Transfer in Perylene-Based Multichromophore Arrays. *Phys. Chem. Chem. Phys.* **2016**, *18* (3), 1712–1719. https://doi.org/10.1039/c5cp06953j.

(21) Wasielewski, M. R. Self-Assembly Strategies for Integrating Light Harvesting and Charge Separation in Artificial Photosynthetic Systems. *Acc. Chem. Res.* **2009**, *42* (12), 1910–1921. https://doi.org/10.1021/ar9001735.

Appendix

N-(4-hydroxyphenyl)-4-bromonaphthalene-1,8-dicarboxymonoimide (3), ^{1}H NMR, DMSO-d$_6$, 400 MHz
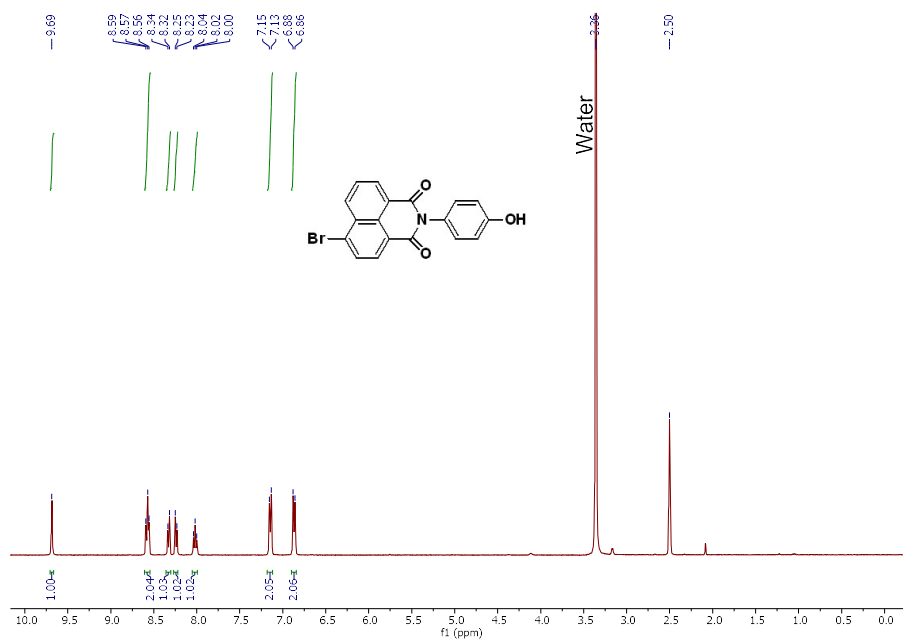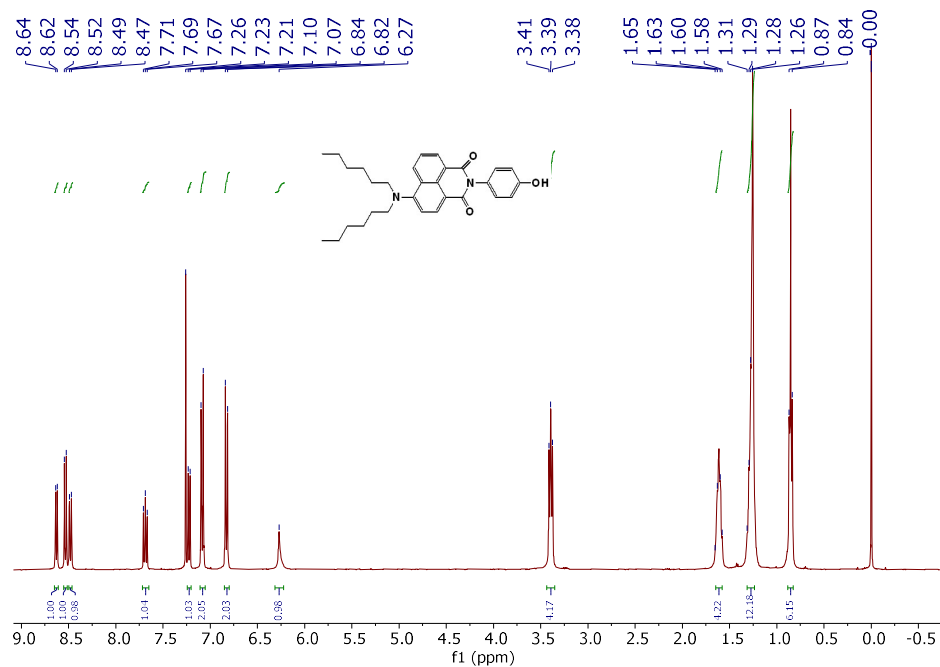

4-hydroxyphenyl)-4-(ethylhexanamine)naphthalene-1,8-dicarboxymonoimide (4), ^{1}H NMR, DMSO-d$_6$, 400 MHz
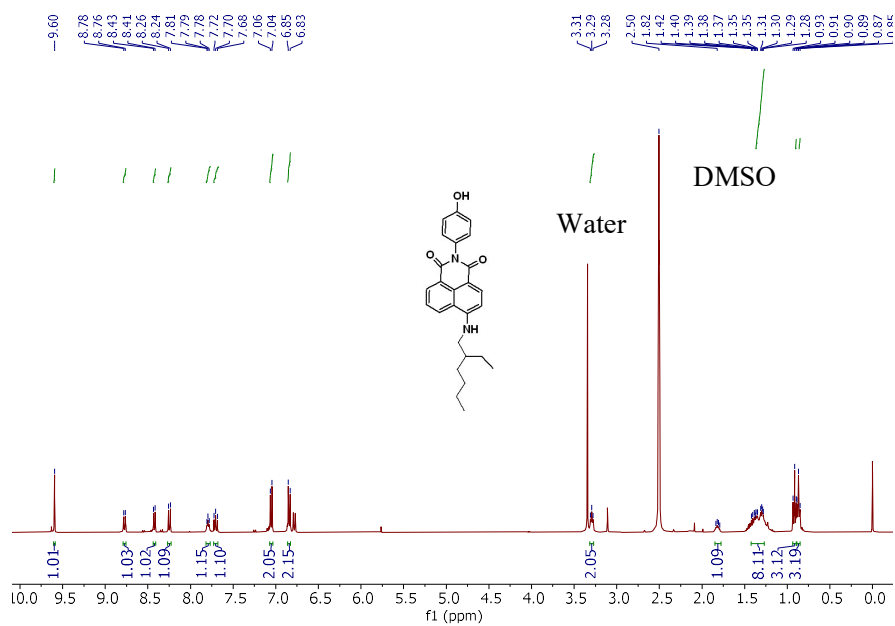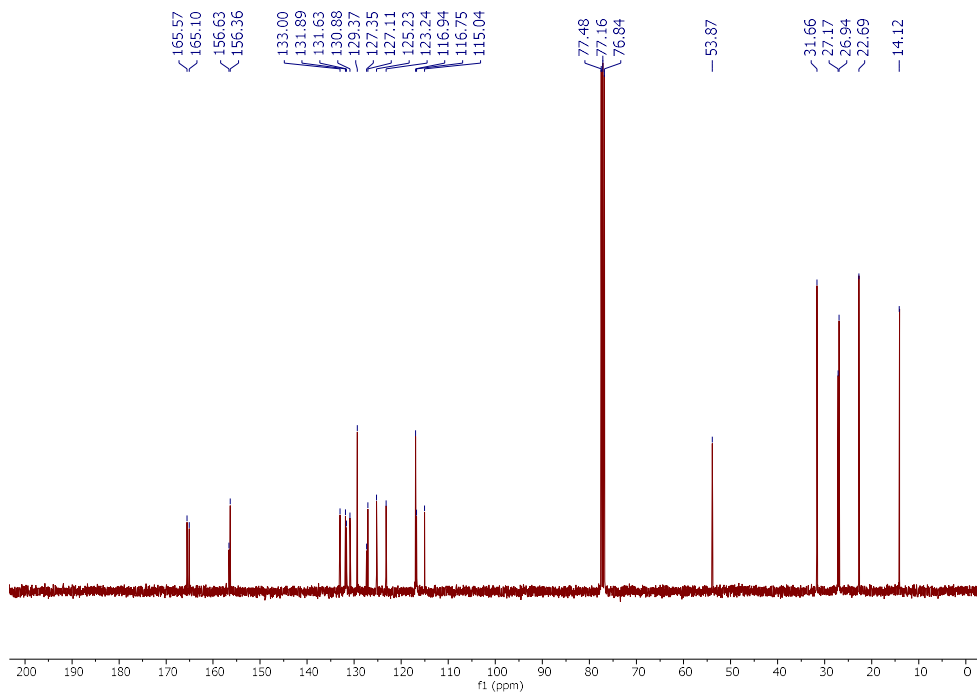
(4-hydroxyphenyl)-4-(dihexylamine)naphthalene-1,8dicarboxy monoimide (5)
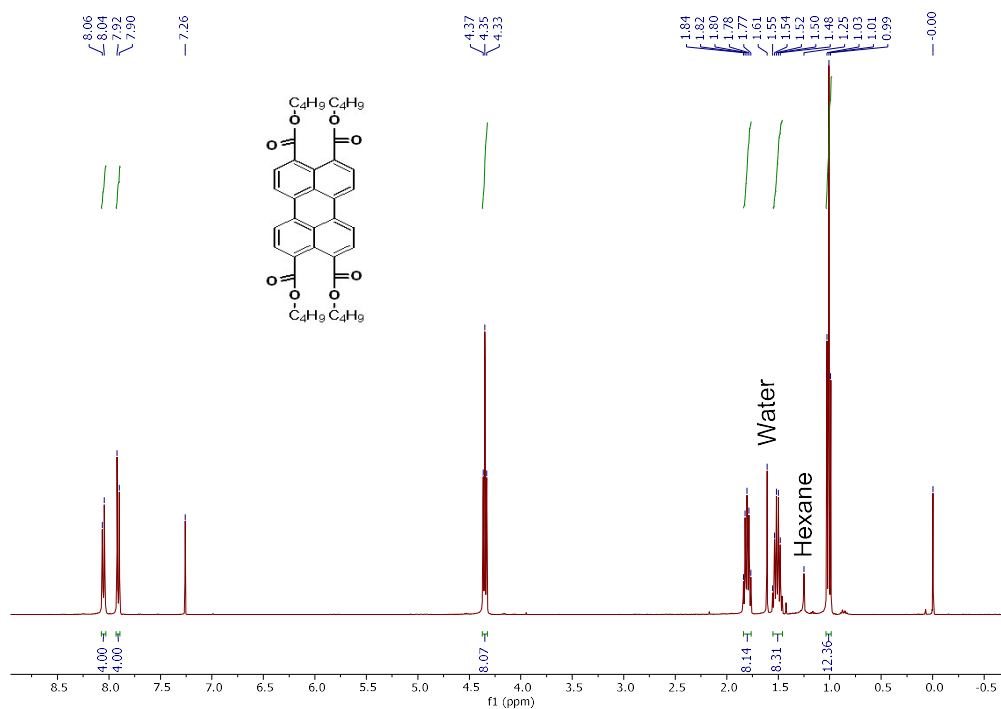
^{1}H NMR, CDCL$_3$, 400 MHz

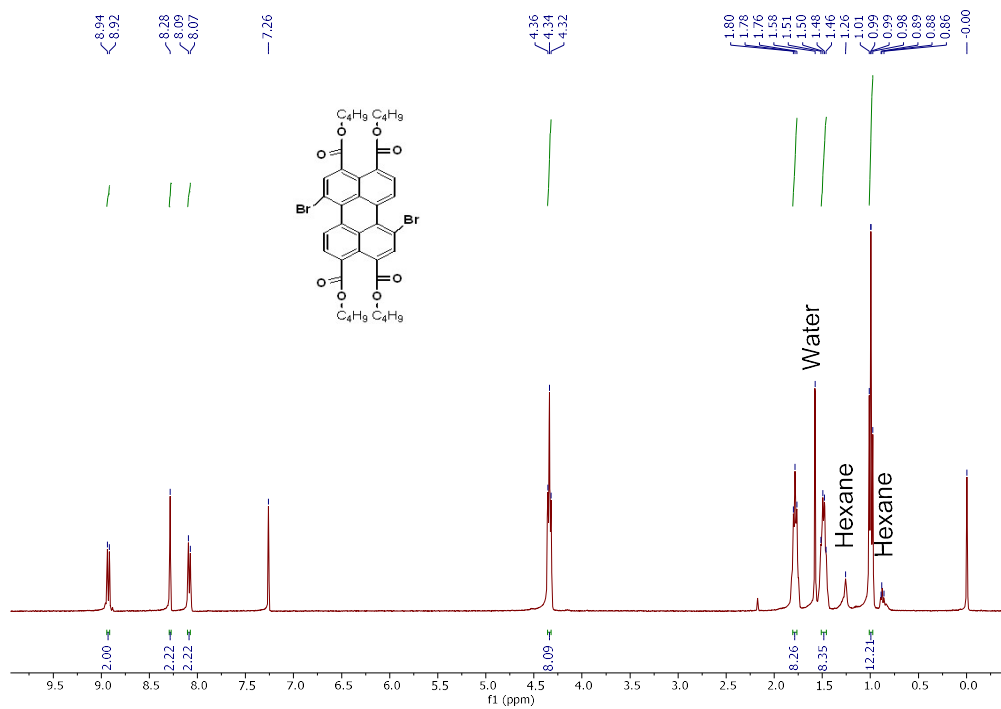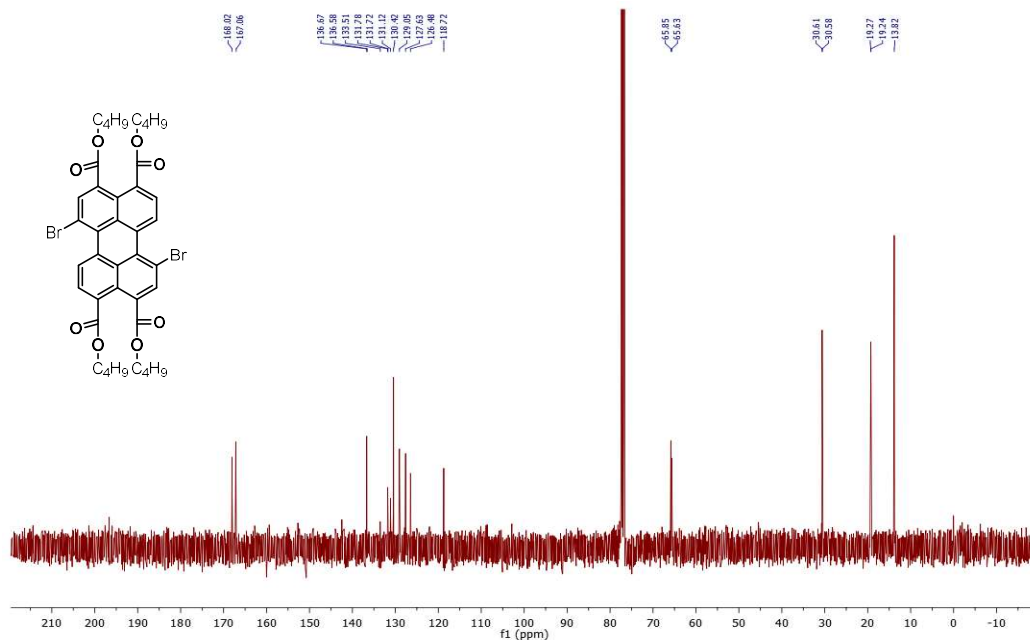**(4-hydroxyphenyl)-4-(dihexylamine)naphthalene-1,8dicarboxy monoimide (5)**

^{13}C NMR, CDCL$_3$, 400 MHz

Perylene-tetracarboxylictetrabutyl ester (7), ¹H NMR, CDCl₃, 400 MHz

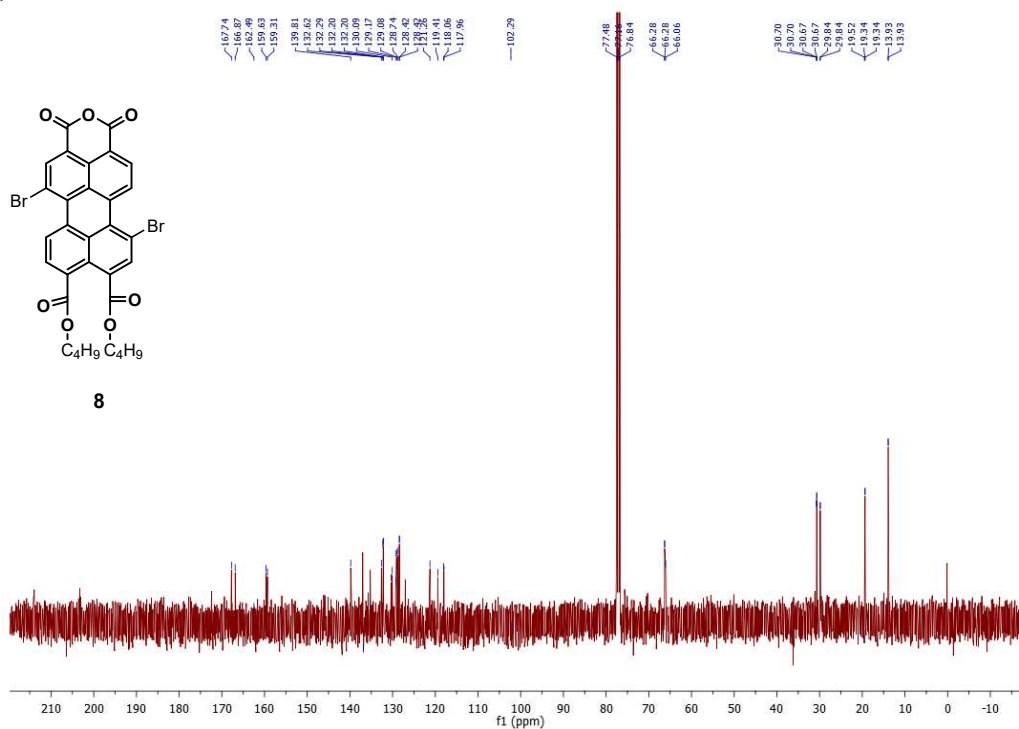**1,7-dibromoperylene-3,4,9,10-tetracarboxylic tetrabutyl ester (8A), ¹H NMR, CDCl₃, 400 MHz**

1,7-dibromoperylene-3,4,9,10-tetracarboxylic tetrabutyl ester (8A), **^{13}C NMR, CDCl₃, 400 MHz**
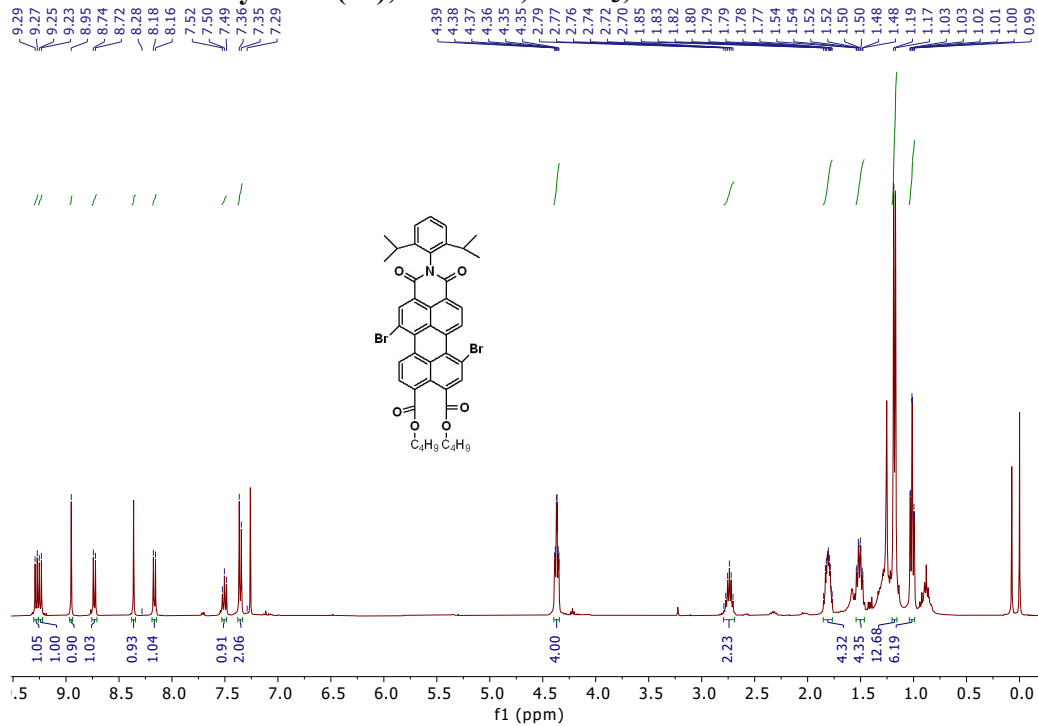

1,7-Dibromoperylene-3,4,9,10-tetracarboxymonoanhydride Dibutylester (9), **^{1}H NMR, CDCl₃, 400 MHz**
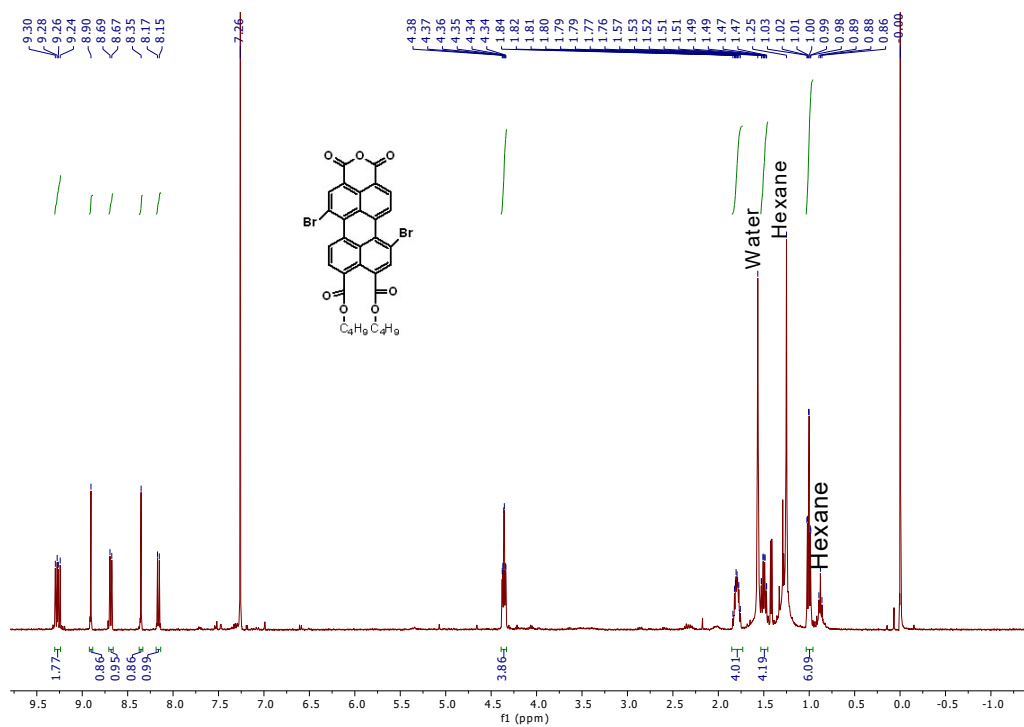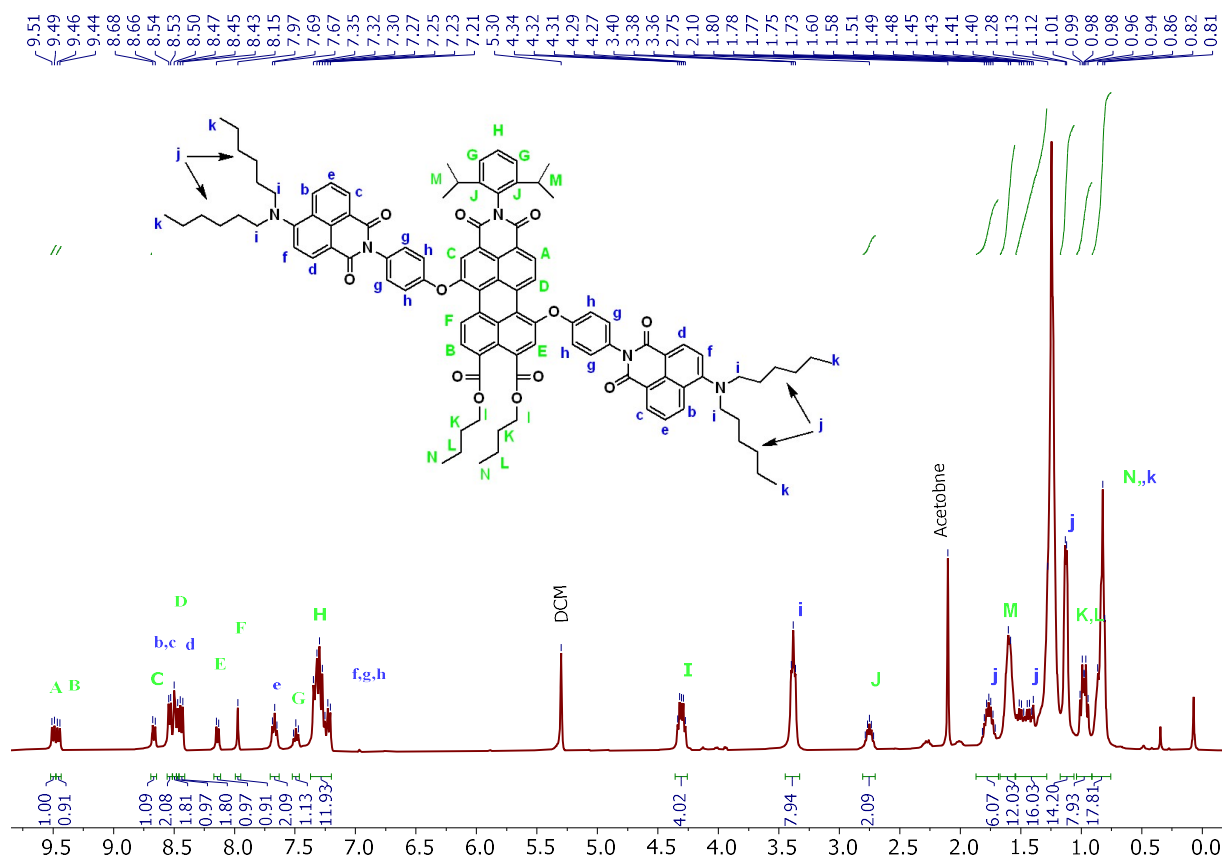
1,7-Dibromoperylene-3,4,9,10-tetracarboxymonoanhydride Dibutylester (9), ^{13}**C NMR, CDCl$_3$, 400 MHz**
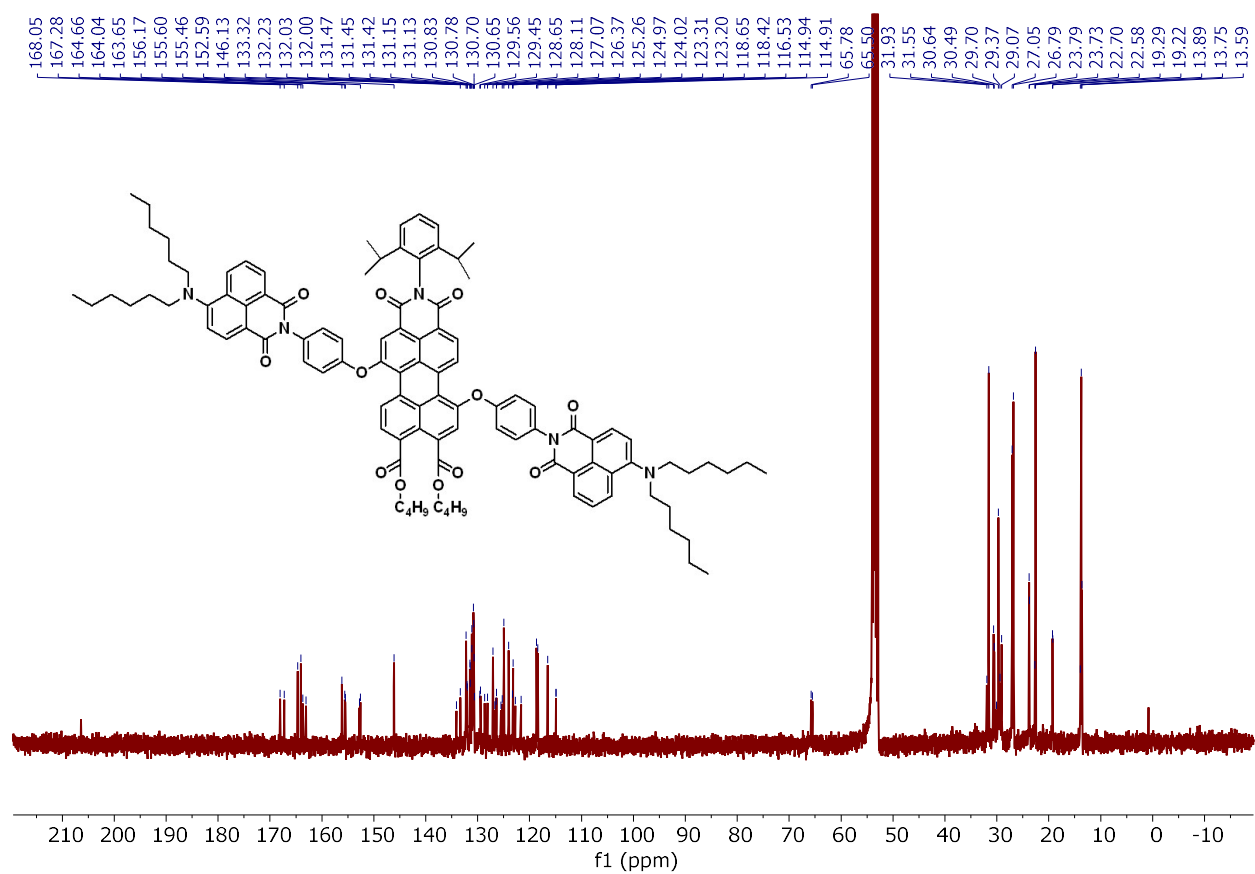

N-(2,6-Diisopropylphenyl)-1,7-dibromoperylene-3,4,9,10-tetracarboxy MonoimideDibutylester (10), ^{1}**H NMR, CDCl$_3$, 400 MHz**
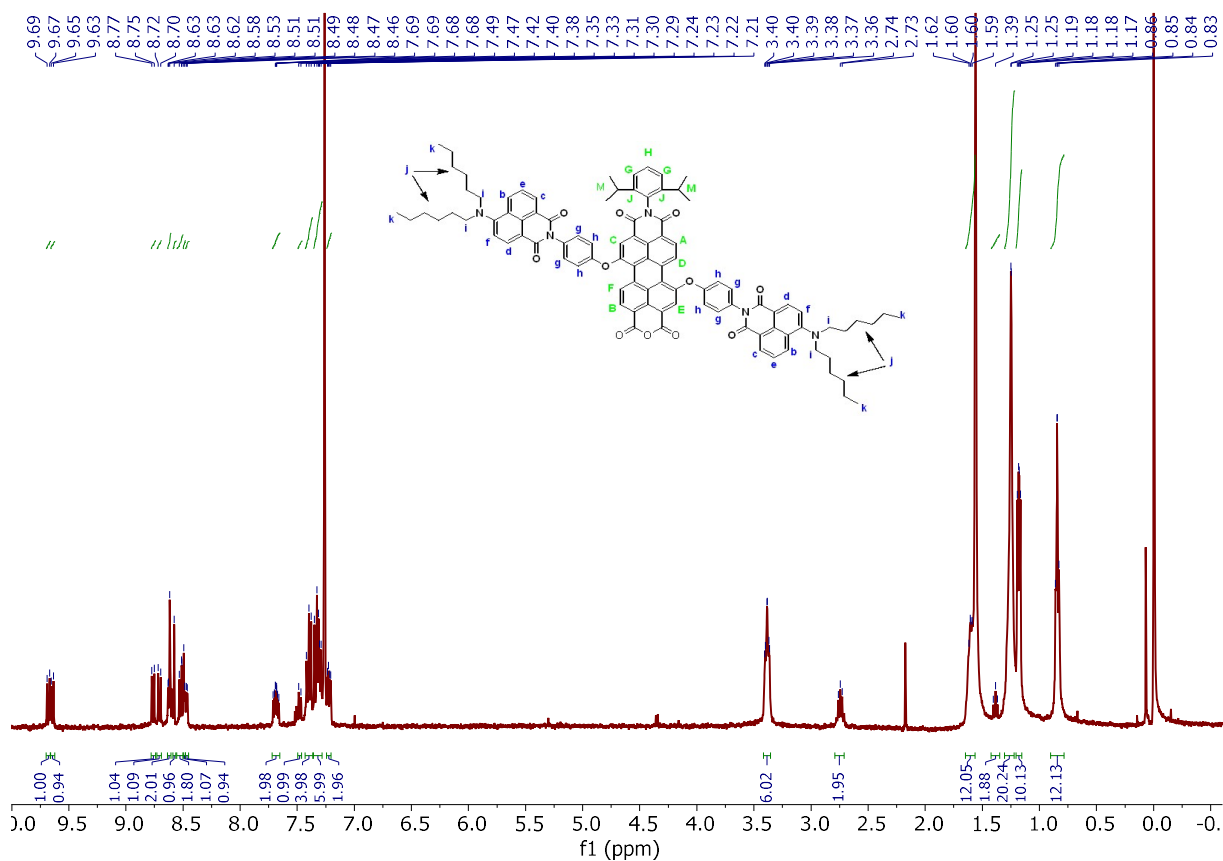
(2,6-diisopropylphenyl)-1,7-bis[N-(pphenyloxy)-(4-(2-ethylhexanamine)-1,8-dicarboxynapthalenemonoimide)]perylene-3,4,9,10-tetracarboxymonoimidedibutylester (11), ¹H NMR, DCM, 400 MHz
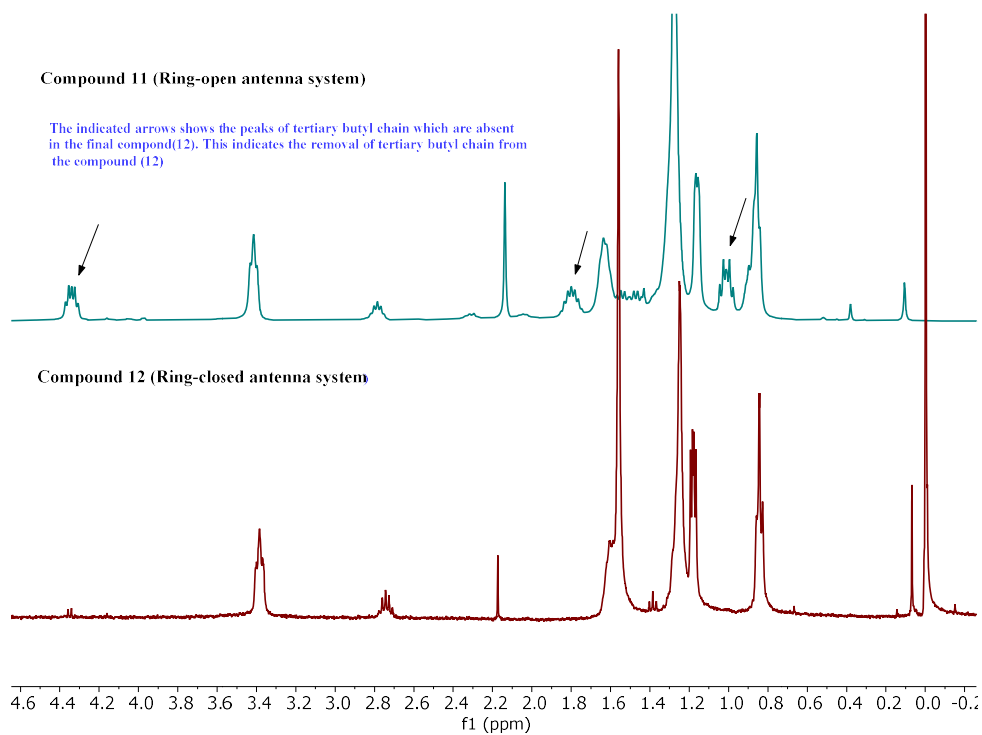
(2,6-diisopropylphenyl)-1,7-bis[N-(pphenyloxy)-(4-(2-ethylhexanamine)-1,8-dicarboxynapthalenemonoimide)]perylene-3,4,9,10-tetracarboxymonoimidedibutylester (11), ^{13}C NMR, CDCl$_3$, 400 MHz

(2,6-diisopropylphenyl)-1,7-bis[N-(pphenyloxy)-(4-(2-ethylhexanamine)-1,8-dicarboxynapthalenemonoimide)]perylene-3,4,9,10-tetracarboxymonoimidedibutylester (12) , ^{1}H NMR, CDCl$_3$, 400 MHz
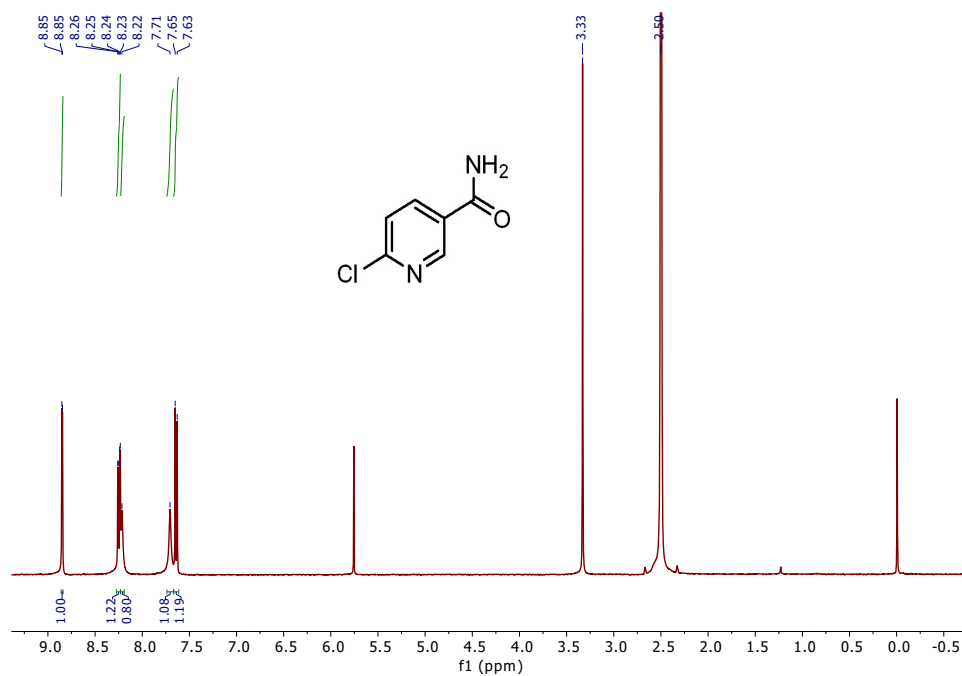
Overlay of compound 11 and 12 (Aliphatic region)

Compound 11 (Ring-open antenna system)

The indicated arrows shows the peaks of tertiary butyl chain which are absent in the final compond(12). This indicates the removal of tertiary butyl chain from the compound (12)

Compound 12 (Ring-closed antenna system)

Overlay of Perylene (10), Naphthalimide (5), and Final ring-close compound (12)

Perylene (10)

Naphthalimide (5)

N-P-N (12)
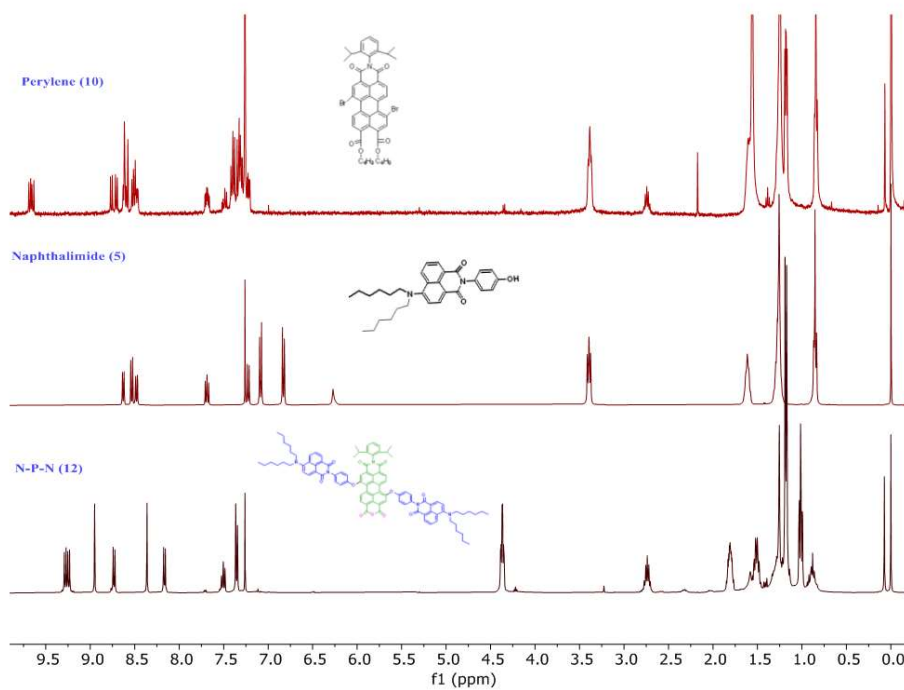
6-chloronicotinamide (14), ^{1}H NMR, DMSO, 400 MHz

Overlay of compound 13 and 14